Myrmecological News
ISSN 1997-3500
myrmecologicalnews.org
Myrmecol. News 30: 27-52 doi: 10.25849/myrmecol.news_030:027 16 January 2020
Original Article

# Unveiling the morphology of the Oriental rare monotypic ant genus *Opamyrma* Yamane, Bui & Eguchi, 2008 (Hymenoptera: Formicidae: Leptanillinae) and its evolutionary implications, with first descriptions of the male, larva, tentorium, and sting apparatus

Aiki Yamada, Dai D. Nguyen, & Katsuyuki Eguchi

**Abstract**

The monotypic genus *Opamyrma* Yamane, Bui & Eguchi, 2008 (Hymenoptera, Formicidae, Leptanillinae) is an extremely rare relictual lineage of apparently subterranean ants, so far known only from a few specimens of the worker and queen from Ha Tinh in Vietnam and Hainan in China. The phylogenetic position of the genus had been uncertain until recent molecular phylogenetic studies strongly supported the genus to be the most basal lineage in the cryptic subterranean subfamily Leptanillinae. In the present study, we examine the morphology of the worker, queen, male, and larva of the only species in the genus, *Opamyrma hungvuong* Yamane, Bui & Eguchi, 2008, based on colonies newly collected from Guangxi in China and Son La in Vietnam, and provide descriptions and illustrations of the male, larva, and some body parts of the worker and queen (including mouthparts, tentorium, and sting apparatus) for the first time. The novel morphological data, particularly from the male, larva, and sting apparatus, support the current phylogenetic position of the genus as the most basal leptanilline lineage. Moreover, we suggest that the loss of lancet valves in the fully functional sting apparatus with accompanying shift of the venom ejecting mechanism may be a non-homoplastic synapomorphy for the Leptanillinae within the Formicidae.

**Key words:** Relictual lineage, China, male genitalia, subterranean ant, venom ejecting mechanism, Vietnam.

Received 30 August 2019; revision received 21 November 2019; accepted 27 November 2019
Subject Editor: Herbert Zettel

*Aiki Yamada (contact author) & Katsuyuki Eguchi, Systematic Zoology Laboratory, Department of Biological Sciences, Graduate School of Science, Tokyo Metropolitan University, 1-1 Minami-Osawa, Hachioji-shi, Tokyo, 192-0397, Japan. E-mail: aiki.ymd@gmail.com*

*Dai D. Nguyen, Systematic Zoology Laboratory, Department of Biological Sciences, Graduate School of Science, Tokyo Metropolitan University, 1-1 Minami-Osawa, Hachioji-shi, Tokyo, 192-0397, Japan; Institute of Ecology and Biological Resources, Vietnam Academy of Science and Technology, 18 Hoang Quoc Viet Road, Cau Giay District, Hanoi, Vietnam.*

## Introduction

The monotypic genus *Opamyrma* Yamane, Bui & Eguchi, 2008 (Hymenoptera, Formicidae, Leptanillinae) is an extremely rare relictual lineage of apparently subterranean ants, so far known only by a few specimens of the worker and queen from Ha Tinh in Vietnam and Hainan in China (Yamane & al. 2008, Chen & al. 2017). This genus was established for a unique species *Opamyrma hungvuong* Yamane, Bui & Eguchi, 2008, which was described based on only two worker specimens discovered from Ha Tinh in Vietnam. The type series was the only known specimens of the genus until a recent rediscovery by Chen & al. (2017) who recovered a single worker and a dealate queen (likely incipient colony) of *O. hungvuong* from Hainan in China. The form of the male and larva, and morphology of some body parts of the worker and queen (e.g., palpi, sting apparatus), and most of biological features of this species remain unknown.

The phylogenetic position of the genus *Opamyrma* had been uncertain until recently. *Opamyrma* was first considered by Yamane & al. (2008) to be a relative of the Afrotropical monotypic genus *Apomyrma* Brown, Gotwald & Levieux, 1971 (but at least one undescribed species is known, see Boudinot 2015) based on some shared morphological characteristics of the worker (the

generic name is the anagram of the name of *Apomyrma*). Yamane & al. (2008) tentatively assigned *Opamyrma* to the subfamily Amblyoponinae together with *Apomyrma* by following definition of the subfamily by Saux & al. (2004). However, recent molecular phylogenetic analysis (Ward & Fisher 2016) indicated a large phylogenetic distance between these two genera, and the phylogenetic position of the two genera, that is, *Apomyrma* as a sister lineage of the Amblyoponinae, and *Opamyrma* as a sister lineage of the subfamily Leptanillinae. Consequently, *Opamyrma* was transferred to the Leptanillinae by Ward & Fisher (2016), whereas the *Apomyrma* is now assigned to own distinct subfamily Apomyrminae by Fisher & Bolton (2016).

The subfamily Leptanillinae is a little-known group of cryptic subterranean ants which are apparently specialized predators. The subfamily has been recovered as one of the most basal extant lineages of ants together with the Amazonian monotypic subfamily Martialinae which is also represented by a single known species, *Martialis heureka* Rabeling & Verhaagh, 2008. However, the position of the root has been controversial (Rabeling & al. 2008, Kück & al. 2011, Branstetter & al. 2017). The most recent molecular phylogenetic analysis by Borowiec & al. (2019) supported Martialinae and Leptanillinae (including *Opamyrma*) together as a clade that is sister to all other extant ants. Therefore, knowledge of *Opamyrma* has great importance for understanding evolutionary history of not only Leptanillinae but also the whole of the Formicidae.

In the last three years, we discovered two *Opamyrma hungvuong* colonies in the course of our field explorations in Guangxi in China and Son La in Vietnam, and had an opportunity to examine the morphology of the worker, queen, male, and larva using an optical microscope and scanning electron microscope (SEM). Herein we provide descriptions and illustrations of the male, larva, and body parts of the worker and queen (including mouthparts, tentorium, and sting apparatus) for the first time. We also highlight morphological characteristics of *Opamyrma* by contrasting it with other ant lineages, particularly other leptanilline genera, *Apomyrma*, and *Martialis*, to provide supporting morphological evidence for the phylogenetic position and novel evolutionary implications.

## Material and methods

**Material examined:** As source materials for morphological examination, the present study used two colony series AKY05vii17-06 (from Guangxi, China containing a total of 57 workers and 12 larvae) and Dai19iii2019-029 (from Son La, Vietnam, containing a total of 18 workers, 18 alate queens, 11 dealate queens, 2 males) that were identified as *Opamyrma hungvuong* Yamane, Bui & Eguchi, 2008 by referring the original description and images of the holotype on AntWeb (CASENT0178347). As many detached wings were included in the ethanol preserved stock from the Son La locale, many of the dealate queens were probably alate when collected. For a details of specimens used for descriptions, see the species account in "Results". Voucher specimens are or will be deposited in the following collections:

| | |
|---|---|
| AKYC | Ant Collection of A. Yamada (currently deposited in the TMUZ). |
| ACEG | Ant Collection of K. Eguchi (currently deposited in TMUZ). |
| GXNU | Insect Collection, Guangxi Normal University, Guilin, Guangxi, China. |
| IEBR | Institute of Ecology and Biological Resources, Vietnam Academy of Science and Technology, Hanoi, Vietnam. |
| MCZC | Museum of Comparative Zoology, Cambridge, Massachusetts, USA. |
| MHNG | Muséum d'Histoire Naturelle, Geneva, Switzerland. |
| TMUZ | Systematic Zoology Laboratory, Tokyo Metropolitan University, Tokyo, Japan. |

**Morphological examination and imaging:** External morphology of the adult body was observed using Nikon SMZ1270 stereomicroscope and an LED epi-illumination device. For transmitted light observations of mouthparts, tentorium and sting apparatus of the worker and queen, male genitalia, and larval head, whole body or focal parts were dissected and slide-mounted with Euparal after cleaning by using the Chelex-TE protocol (for detail see Yamada & Eguchi 2016); and then slide-mounted specimens were observed using Nikon Eclipse E600 microscope. The worker, queen, and larva were also observed and photographed using scanning electron microscope (SEM), JEOL JSM-6510. Ethanol-preserved specimens were dissected, dried and then mounted on specimen stubs and coated with platinum before SEM observation; the t-butyl alcohol freeze-dry method (Inoue & Osatake 1988) was used for preparation of larval specimens. Source images for focus stacking and measurements were taken by a Canon EOS Kiss X9 digital camera attached to a Nikon AZ100 stereomicroscope (for dry-mounted specimens) or Nikon Eclipse E600 microscope (for slide-mounted specimens). Multi-focused images were produced by Helicon Focus Pro 7.5.0 (Helicon Soft Ltd., Ukraine), and then improved using the retouching function of Helicon Focus. The color balance, contrast, and sharpness of the images were adjusted using Adobe Lightroom Classic CC 8.1 and GIMP 2.10 (The GIMP Development Team, available at http://www.gimp.org/).

The morphological terminology follows Gotwald (1969), Keller (2011), Richter & al. (2019), and Liu & al. (2019) for general morphology of the worker, Kugler (1978) for sting apparatus, Kubota & al. (2019) for tentorium, and Boudinot (2013, 2015) for general morphology of the male and queen. For wing terminology, the style in Boudinot (2015) is followed: Brown & Nutting (1949) for wing venation, Mason (1986) for wing vein development, and Yoshimura & Fisher (2011) for cellular terminology with the modifications proposed in Boudinot & al. (2013); the wing venation typification system presented by Ogata (1991) is also used.


Fig. 1: General habitus of *Opamyrma hungvuong* worker, nontype (AKY05vii17-06, China, Guangxi). (A) head in full-face view; (B) head in anteroventral view; (C) body in lateral view; (D) body in dorsal view. Abbreviations: Occ = occipital carina; Lbr = labrum; Pgr = postgenal ridge.

The following parts of bodies were measured using ImageJ 1.52a (National Institute of Mental Health, USA, available at http://imagej.nih.gov/ij/), and then indices were calculated.

CI Cephalic index: HW / HL × 100.
EI Eye index: EL / HW × 100.
EL Eye length: maximum length of major axis of eye in lateral view (for queen and male only).
HL Head length: minimal length of cranium in full-face view, measured from the anteromedian margin of clypeus to the posterior margin of cranium.
HW Head width: maximum width of cranium in full-face view (excluding eyes).
MFI Metafemur index: MFL / HW × 100.
MFL Metafemur length: the maximum length of the metafemur, measured in dorsal view.
OI Ocellus index: OL / HW × 100.
OL Ocellus length: maximum length of major axis of median ocellus (for queen and male only).
PTH Petiolar height: maximum height of petiole in lateral view.
PTI Petiolar index: PTW / PTL × 100.
PTL Petiolar length: minimal length of petiole in lateral view, measured from posterodorsal corner of anterior articulation to posterior margin of posterior peduncle, inside which the helcium articulates.
PTW Petiolar width: maximum width of petiole in dorsal view.
PW Pronotal width: the maximum width of the pronotum in dorsal view.
SI Scape index: SL / HW × 100.
SL Scape length: maximum length of antennal scape excluding basal condylar bulbus.
WL Weber's length of mesosoma: maximum diagonal distance of mesosoma in lateral view, measured from the point at which the pronotum meets the cervical shield to the posteroventral corner of propodeum.

## Results

### *Opamyrma hungvuong*
**Yamane, Bui & Eguchi, 2008**
(Figs. 1 - 15)

**Non-type material examined: China:** 25 workers, 6 larvae (colony ID: AKY05vii17-06), Guangxi, Guilin, Huaping National Nature Reserve, 25.57° N, 109.94° E, ca. 1000 - 1500 m above sea level (a.s.l.), collected from soil under stone on forest floor, coll. A. Yamada, 5 July 2017 (AKYC, ACEG, GXNU, MCZC, MHNG). **Vietnam:** 3 workers, 2 alate queens, 5 dealate queens, 2 males (colony ID: Dai19iii2019-029), Son La, Ta Xua Nature Reserve, Bac Yen, Hang Dong, 21.3158° N, 104.5213° E, 1533 m a.s.l., collected from soil on forest floor, coll. D. D. Nguyen, 14 March 2019 (AKYC, ACEG, IEBR, MCZC, MHNG).

**Diagnosis:** The female (worker and queen) of the unique species is easily recognizable by the following combination of characteristics: 1) occipital carina virtually uninterrupted and anteriorly located before the posterior margin of cranium; 2) outer face of labrum bears numerous peg-like setae; 3) waist 1-segmented; 4) petiole without distinct anterior peduncle; 5) tergosternal fusion of petiole present only anteriorly; 6) gaster elongated and flattened laterally, with distinct presclerites in abdominal segment IV. The male may be recognizable by the following combination of characteristics: 1) mandible reduced and nub-like; 2) wing venation reduced (Ogata's venation type IVb) with only three closed cells, that is, basal, subbasal, and discal cells; 3) propodeal lobes inconspicuous; 4) waist 1-segmented; 5) petiole not tergosternally fused; 6) pygostyli absent; 7) abdominal sternite IX without prongs or teeth, and with posteromedian lobe; 8) genitalia conspicuous with extremely elongate telomere directed ventrad in repose.

**Measurements and indices: Worker:** CI 76 - 82; HL 0.62 - 0.71 mm; HW 0.48 - 0.54 mm; MFI 91 - 96; MFL 0.44 - 0.50 mm; PTH 0.28 - 0.38 mm; PTI 46 - 50; PTL 0.42 - 0.55 mm; PTW 0.21 - 0.27 mm; PW 0.35 - 0.43 mm; SI 64 - 71; SL 0.33 - 0.38 mm; WL 1.01 - 1.18 mm (n = 7).

**Queen:** CI 78 - 79; EI 24 - 25; EL 0.17 mm; HL 0.86 - 0.87 mm; HW 0.68 mm; MFI 89 - 92; MFL 0.61 - 0.63 mm; OI 8 - 9; OL 0.05 - 0.06 mm; PTH 0.48 - 0.49 mm; PTI 50 - 56; PTL 0.69 - 0.70 mm; PTW 0.35 - 0.38 mm; PW 0.58 - 0.60 mm; SI 67 - 69; SL 0.45 - 0.47 mm; WL 1.58 - 1.63 mm (n = 3).

**Male:** CI 99 - 106; EI 53 - 56; EL 0.33 mm; HL 0.59 mm; HW 0.58 - 0.62 mm; MFI 104 - 109; MFL 0.64 - 0.65 mm; OI 15; OL 0.09 - 0.10 mm; PTH 0.36 - 0.37 mm; PTI 92 - 99; PTL 0.34 - 0.36 mm; PTW 0.31 - 0.35 mm; PW 0.53 mm; SI 19; SL 0.11 - 0.12 mm; WL 1.48 - 1.49 mm (n = 2).

**Redescription: Worker (Figs. 1 - 9):** C r a n i u m. In full-face view subrectangular, longer than wide, with slightly convex lateral margin and slightly concave posterior margin, in lateral view, flattened dorsoventrally. Median longitudinal cephalic carina absent. Frontal carina and lobes absent. Occiput extended anteriorly to have distinct dorsal, lateral, and ventral face, delimited anteriorly by distinct occipital carina ("Occ" in Figs. 1A - B, 2B, 4C; = "preoccipital carina" in the original description); the carina virtually uninterrupted, forming a V-shaped angle at the middle of the venter (arrow in Fig. 2B). Postgenal ridge ("Pgr" in Figs. 1B, 4C) externally visible as a dark line running on the ventral midline, ending a little before the level of occipital carina (the dark line was mentioned as "median furrow" in the original description, but the ventral midline is not furrowed as seen in Fig. 2B). Hypostomal process ("Hysp" in Fig. 2B, D) conspicuous, in lateral view broad with rounded apex. Eye and ocelli completely absent. Antennal socket completely exposed in full-face view, directing almost dorsad, located in a large, roundly excavated area of which anterior wall is steep a little behind the anterior margin of clypeus; the area not clearly defined posteriorly. Antennal torulus distinct, simple annular, located distant from anterior clypeal margin, posterolaterally surrounded by deep tear-

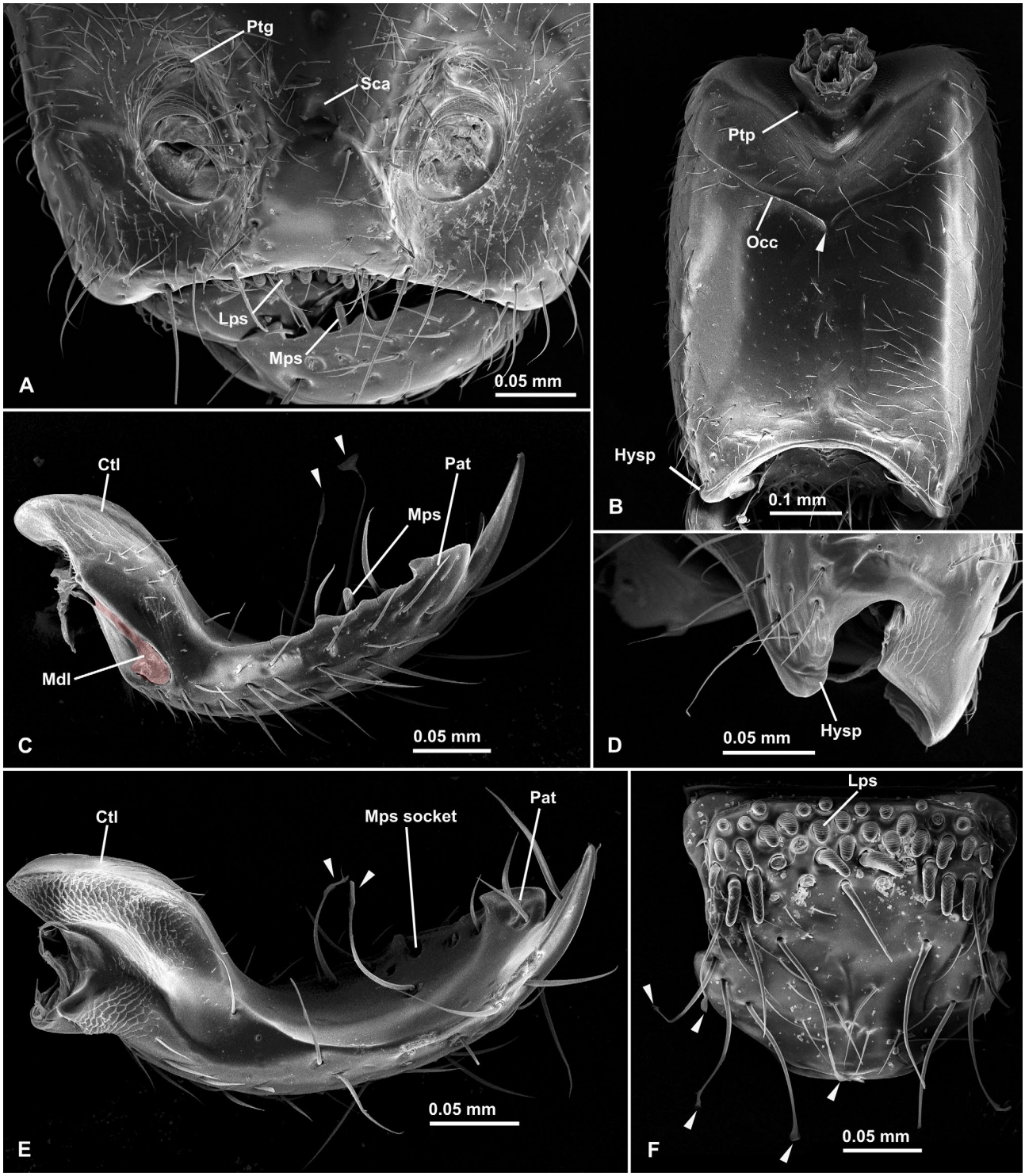


Fig. 2: Scanning electron microscope images of cephalic parts of *Opamyrma hungvuong* worker, nontype (AKY05vii17-06, China, Guangxi). (A) anterior part of head in frontal view; (B) cranium in ventral view; (C) right mandible in dorsal view; (D) right hypostomal process in lateral view; (E) left mandible in ventral view; (F) labrum in outer view. Abbreviations: Ctl = canthellus; Hysp = hypostomal process; Occ = occipital carina; Lbr = labrum; Lps = labral peg-like seta; Mdl = mandalus; Mps = mandibular peg-like seta; Pat = preapical tooth; Ptg = peritorular groove; Ptp = posterior tentorial pit; Sca = supraclypeal area.

drop-shaped peritorular groove ("Ptg" in Figs. 2A, 4A - B; the term "peritorular groove" is borrowed from Richter & al. 2019). Anterior tentorial pit not externally visible (see tentorium description below). Posterior tentorial pit ("Ptp" in Figs. 2B, 4C) located laterally to postocciput. Median portion of clypeus rather clearly divided into anterior steep slope and posterior horizontal area that is raised dorsad and posteriorly roundly delimited by a continuous steep

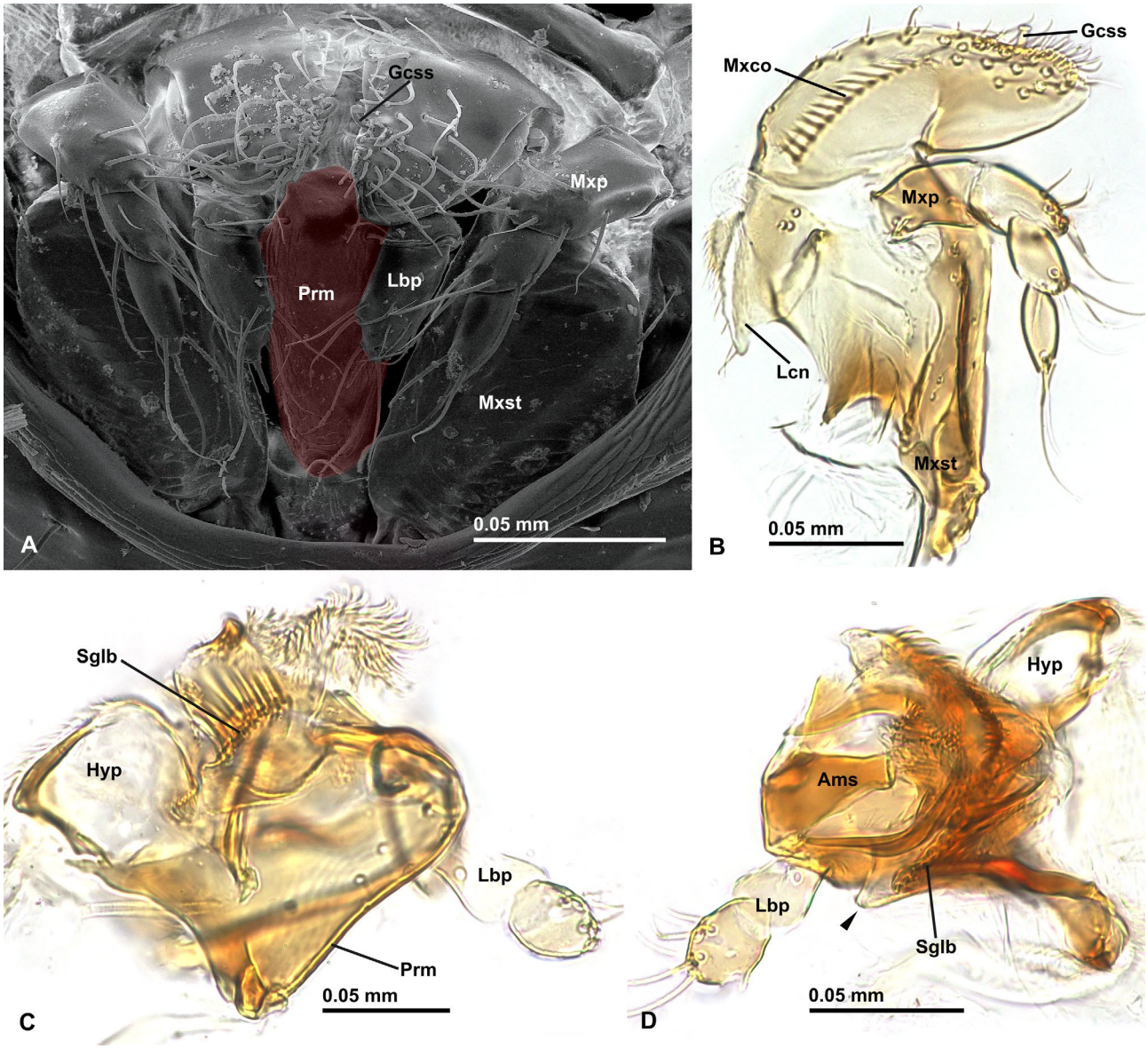


Fig. 3: Maxillolabial complex of *Opamyrma hungvuong* worker, nontype (AKY05vii17-06, China, Guangxi). (A) Scanning electron microscope image of maxillolabial complex in ventral view, labrum removed; (B) right maxilla in outer view; (C) labium in lateral view; (D) labium in dorsal view. Abbreviations: Ams = anteromedian sclerite; Gcss = galeal crown's stout seta; Hyp = hypopharynx; Lbp = labial palp; Lcn = lacinia; Mxco = maxillary comb; Mxp = maxillary palp; Mxst = maxillary stipes; Prm = prementum; Sglb = subglossal brush.

declivity; posterior area broadly inserted between antennal sockets, nearly reaching the level of posterior margin of antennal torulus; supraclypeal area ("Sca" in Fig. 2A) small, subtriangular; median longitudinal clypeal carina absent; lateral portion of clypeus in front of antennal socket very narrow anteroposteriorly: posterior limit of lateral portion of clypeus externally not obvious, but internal line that might be paroculoclypeal sulcus (dashed line in Fig. 4A) tracing the anterior outline of excavated area around antennal socket is recognized under transmitted light microscope; anterior clypeal margin broadly concave without any peg-like setae or cuticular denticles.

M o u t h p a r t s. Mandible short and sublinear, strongly curved near the distal end of mandalus, with long but somewhat bluntly tapering apical tooth followed by a broad trapezoidal preapical tooth ("Pat" in Fig. 2C, E; in the original description, the preapical tooth was mentioned as "trapezoidal lobe" that was interpreted as fusion of two preapical teeth, but it could well be a single preapical tooth corresponding in location to, for example, *Apomyrma*, †*Gerontoformica* Nel & Perrault, 2004, and *Prionopelta* Mayr, 1866) and three or four inconspicuous teeth; ventral face with a single peg-like seta ("Mps" in Fig. 2A, C, E; the seta morphology is similar to that of labrum) which is located near the base of the second and third inconspicuous teeth of the masticatory margin, and two long apically spatulate setae (arrows in Fig. 2C, E); trulleum apparently absent; canthellus ("Ctl" in Fig. 2C, E)

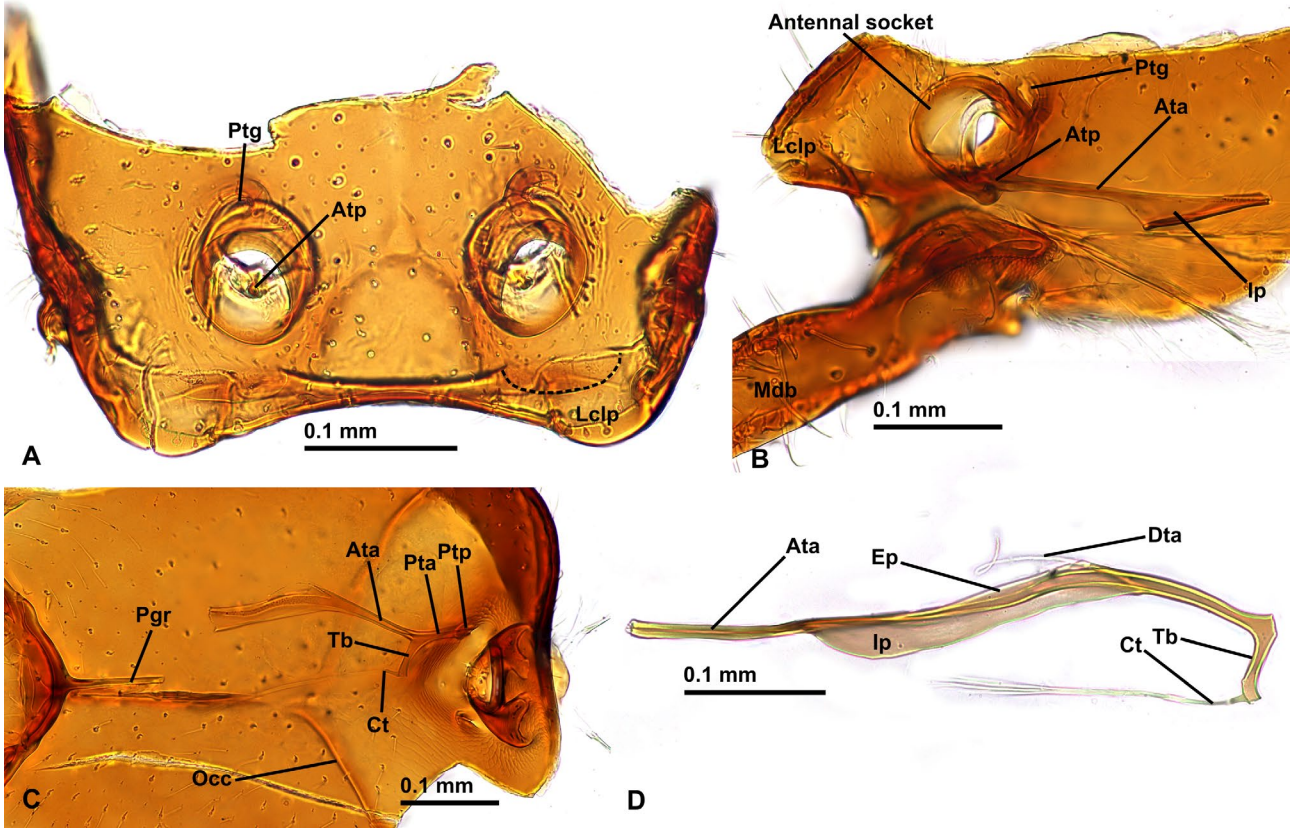


Fig. 4: Tentorium of *Opamyrma hungvuong* worker, nontype (AKY05vii17-06, China, Guangxi). (A) anterior part of dorsal sclerite of cranium in dorsal view; (B) part of dorsal sclerite of cranium around right antennal socket with anterior part of tentorium, in inner ventral view; (C) part of ventral sclerite of cranium with posterior part of tentorium in inner dorsal view; (D) right half of tentorium in dorsal view (lacking posterior tentorial arm). Abbreviations: Ata = anterior tentorial arm; Atp = anterior tentorial pit; Ct = corpotendon; Dta = dorsal tentorial arm; Ep = external plate; Ip = internal plate; Lclp = lateral portion of clypeus; Mdb = mandible; Occ = occipital carina; Pgr = postgenal ridge; Pta = posterior tentorial arm; Ptg = peritorular groove; Ptp = posterior tentorial pit; Tb = tentorial bridge.

less-defined, not differentiated from the basal margin of mandible; mandalus ("Mdl" marked by red color in Fig. 2C) elongate and narrow club-shaped (it is visible as whitish membranous area in dry specimen under an optical microscope, and it was misinterpreted as trulleum in the original description). Labrum (Fig. 2F, "Lbr" in Fig. 1B) large, entirely concealing prementum ("Prm" in Fig. 3A, C) and maxillary stipes ("Mxst" in Fig. 3A - B) when mouthparts retracted, almost as long as wide, with rounded distal margin (median cleft absent); labral tuberculi absent; basal third of the outer face bearing numerous peg-like setae that are arranged regularly but not in strict transverse rows ("Lps" in Fig. 2A, F); distal area of the outer face with at least five pairs of long apically spatulate setae (halves of the pairs are indicated by arrows in Fig. 2F) that are regularly arranged. Maxilla with conspicuous maxillary comb ("Mxco" in Fig. 3B); transverse stipital groove absent; galeal comb absent; galeal crown flattened with a series of thick apically rounded (not spatulate) setae, one of which is particularly stout ("Gcss" in Fig. 3A - B), without ventral comb; lacinia ("Lcn" in Fig. 3B) small subtriangular, with relatively acute apex; lacinial comb present, composed of short thin setae; maxillary palp ("Mxp" in Fig. 3A - B) 4-segmented, becoming shorter and narrower apically; apical segment with bluntly tapering apex. Premental shield (ventral surface of prementum, marked by red color in Fig. 3A) convex oblong in ventral view, without transverse premental groove. Labium in dorsal view with conspicuous anteromedian sclerite ("Ams" in Fig. 3D) that is apparently dorsal extension of prementum; base of subglossal brush ("Sglb" in Fig. 3C - D) forming strong anterolateral projection in dorsal view (arrow in Fig. 3D); paraglossa unrecognizable in our observation; labial palp ("Lbp" in Fig. 3A, C - D) 2-segmented; second segment about as long as first segment, with rounded apex.

T e n t o r i u m. Anterior tentorial arm ("Ata" in Fig. 4B - D) originated from endoskeletal structure of antennal socket; anterior tentorial pit apparently located on medioventral wall of antennal socket ("Atp" in Fig. 4A - B). Buttress-like extension absent. Internal plate ("Ip" in Fig. 4B, D) relatively narrow but much broader than external plate ("Ep" in Fig. 4D), with rounded anterodistal corner. Dorsal tentorial arm ("Dta" in Fig. 4D) distinct, with long branch-like apical part. Tentorial bridge ("Tb" in Fig. 4C - D) thin

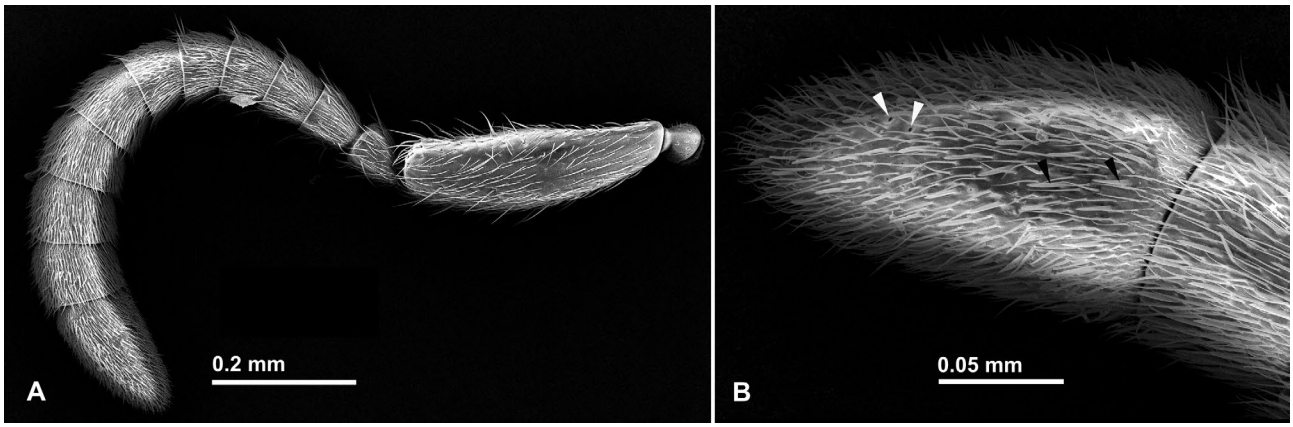


Fig. 5: Scanning electron microscope images of antenna of *Opamyrma hungvuong* worker, nontype (AKY05vii17-06, China, Guangxi). (A) entire right antenna in dorsal view; (B) apical antennomere in dorsal view.

tubular. Corpotendon ("Ct" in Fig. 4C - D) long. Posterior tentorial arm ("Pta" in Fig. 4C) thin tubular.

A n t e n n a. Antenna 12-merous, gradually incrassate from antennomeres II to XII (Fig. 5A). Antennal scape, when laid backward, extending past midlength of cranium, flattened dorsoventrally, narrowed toward base, without distinct basal flange distal to bulbus; antennomere II subconical bead-like, in dorsal view strongly narrowed at base, slightly longer than wide; antennomore III slightly longer than wide and narrowed basally; antennomeres IV and V almost as long as wide; antennomeres VI - XI wider than long; apical antennomere longer than wide and bluntly pointed at apex. Apical antennomere, with at least two types of sensilla recognizable: basiconic (black arrows in Fig. 5B), and trichodic ones; trichodic sensilla become small on basal marginal area; pit-like structures that might be coeloconic / ampullaceous sensilla or socket of broken basiconic / trichodic sensilla also recognizable (white arrows in Fig. 5B). Scape bulbus hemispherical with short tubular neck; anterior basal margin of the bulbus apparently without a distinct notch.

M e s o s o m a. Mesosoma slender and consisting of two distinct portions, prothorax and meso-metathoracico-propodeal complex, which is oblong and slightly longer and narrower than pronotum and almost parallel-sided in dorsal view: articulation between prothorax and mesothorax unfused and fully flexible in fresh condition. Pronotum longer than wide in dorsal view, with slightly convex dorsal face that roundly continues to lateral face; anterior slope short and steep. Propleurae unfused relative to one another, but are strongly attached along the ventral midline. Procoxal cavity ("Pcc" in Fig. 6D, F) as small as meso- and metacoxal cavities, in ventral view bounded anteriorly by propleuron and laterally and posteriorly by prosternum (virtually not bounded by pronotum). Dorsum of anterior articulatory area of mesonotum (inserted under the pronotum, marked by blue color in Fig. 6B - C) posteriorly delimited by deep narrow transverse groove ("Msg", marked by red color in Fig. 6B - C) which continues along the ventral margin of mesopleuron. Mesonotal spiracle unrecognizable in our observation. Notopleural suture of mesothorax absent. Longitudinal mesopleural sulcus absent. Metanotal groove absent. Mesometapleural suture present as weak groove. Metanotal spiracle ("Mtsp" in Fig. 6A) small and apparently closed, located high on lateral face. Propodeum with rather flat dorsum and steep posterior face; posterior face roundly continues to dorsal and lateral faces without any delimiting carina. Propodeal spiracle located relatively low on the lateral face of propodeum. Outline of metapleural gland bulla conspicuously recognized through cuticle under natural lighting, subcircular, occupying posterior two-fifths of ventrolateral part of the pleuron; metapleural gland orifice ("Mgo" in Fig. 6E) narrow slit-like, located in the lower posterior corner of the metapleuron; metapleural longitudinal flange ("Mlf", marked by green color in Fig. 6E) anteroposteriorly long, projecting laterad and overhanging (but not concealing) metapleural gland orifice. Ventral part of metapleuron below the orifice also laterally produced to form longitudinal flange. Propodeal lobes ("Pdl" in Fig. 6C - E) weakly present, low and round. Anteroventral face of mesopectus with distinct median carina and submedial deep subrectangular depressions that accommodate the forecoxae; posterior remaining face just medially weakly raised without forming distinct median carina. Mesosternal pit present ("Mstp" in Fig. 6D). Metasternal pit apparently absent. Meso- and metacoxal cavities small, fully closed with a complete cuticular annuli surrounding the cavities; metacoxal cavity separated from propodeal foramen by a cuticular band.

L e g s. Relatively broad gap present between pro- and mesocoxae. Metacoxal dorsum unarmed. Profemur broader than meso- and metafemur. Protibia broader than meso- and metatibia. Anterior face of protibia without "protibial anterior sulcus" sensu Keller (2011). The calcar of the strigil ("Ca" in Fig. 7A - C) fully pectinated; basal one third of the calcar bearing narrow unnotched lamina (arrow in Fig. 7B); anterior surface with brush that is composed of dense seta-like cuticular projections; posterior surface with sparse seta-like cuticular projections. Pos-

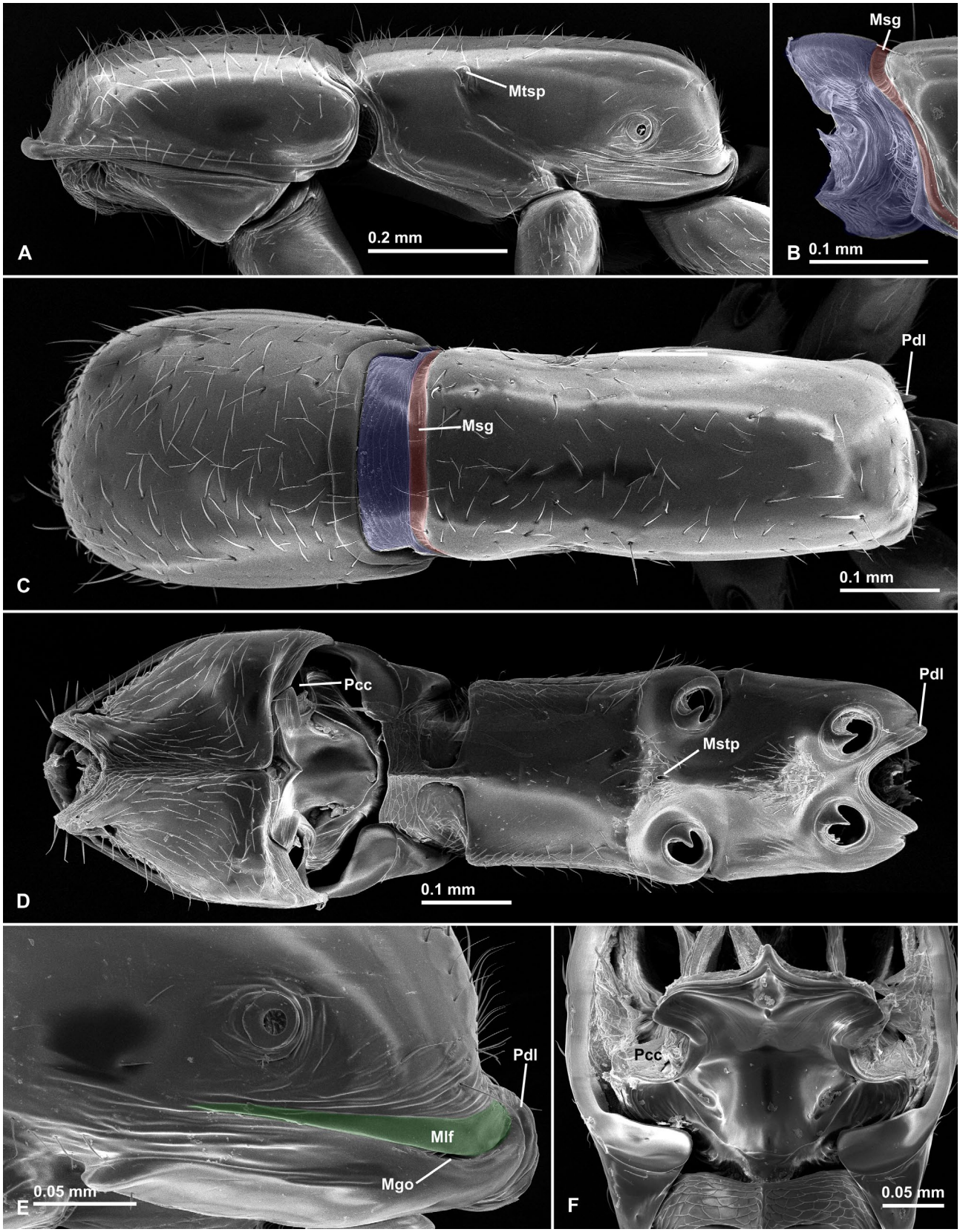


Fig. 6: Scanning electron microscope images of mesosoma of *Opamyrma hungvuong* worker, nontype (AKY05vii17-06, China, Guangxi). (A) whole mesosoma in lateral view; (B) anterior articulation of mesonotum in lateral view, prothorax removed; (C) whole mesosoma in dorsal view; (D) whole mesosoma in ventral view, all legs removed; (E) metapleuron and propodeum in lateral view; (F) prosternite in ventral view, propleurae and prolegs removed. Abbreviations: Mgo = metapleural gland orifice; Mlf = metapleural longitudinal flange; Msg = mesonotal groove; Mstp = mesosternal pit; Mtsp = metanotal spiracle; Pcc = procoxal cavity; Pdl = propodeal lobe.

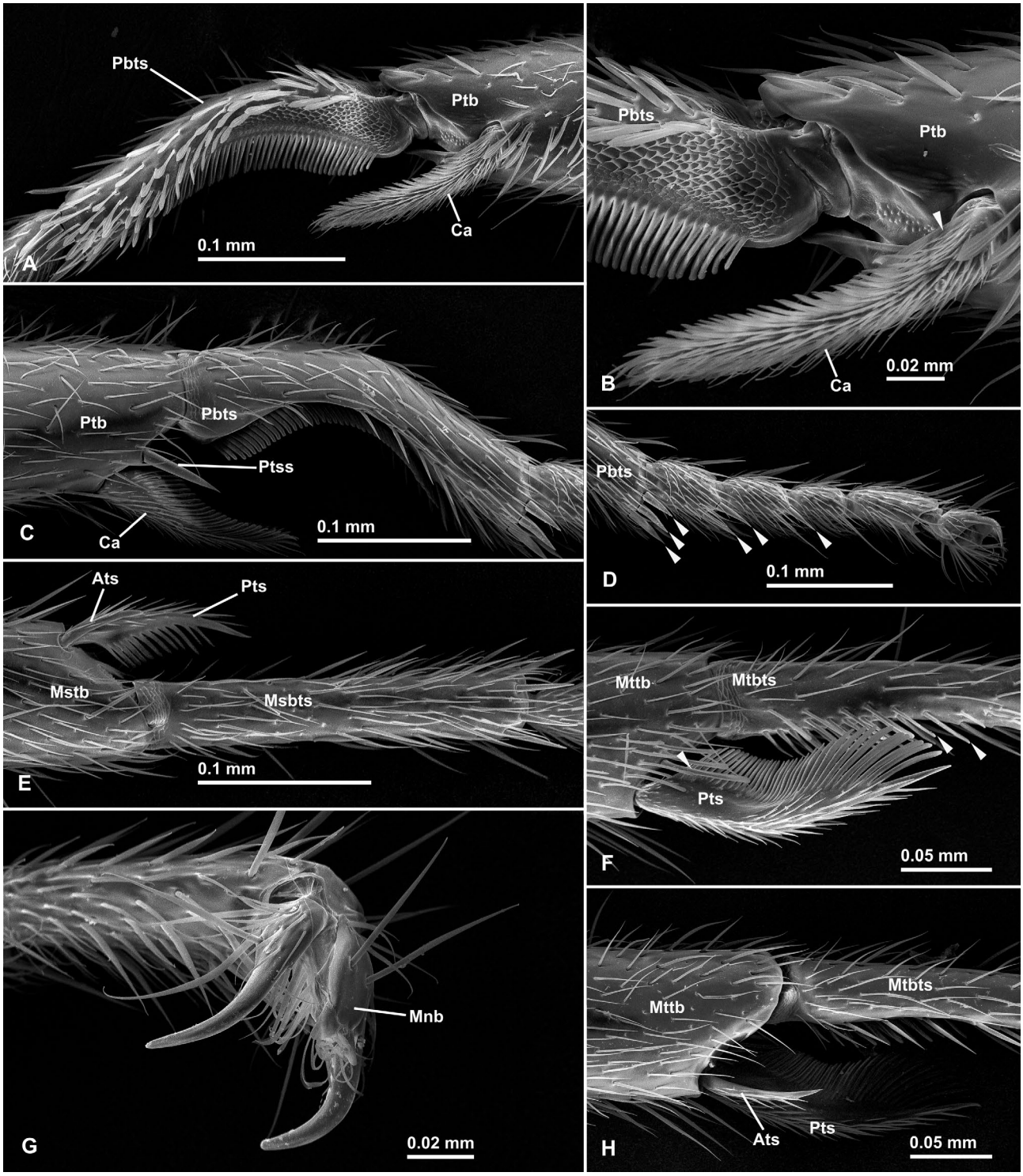


Fig. 7: Scanning electron microscope images of legs of *Opamyrma hungvuong* worker, nontype (AKY05vii17-06, China, Guangxi). (A) strigil of right proleg in anterior view; (B) calcar of strigil of right proleg in anterior view; (C) strigil of right proleg in posterior view; (D) distitarsus of right proleg in posterior view; (E) tibial spurs and basitarsus of right mesoleg in anterior view; (F) tibial spurs and basitarsus of right metaleg in posterior view; (G) pretarsal claws of right metaleg in posteroventral view; (H) tibial spurs of left metaleg in anterior view. Abbreviations: Ats = anterior spur; Ca = calcar; Pts = posterior spur; Ptb = protibia; Pbts = probasitarsus; Ptss = protibial stout seta; Mnb = manubrium; Mstb = mesotibia; Msbts = mesobasitarsus; Mttb = metatibia; Mtbts = metabasitarsus.

terodistal apex of protibia with a single stout seta ("Ptss" in Fig. 7C), located close to the insertion of the calcar of the strigil. Meso- and meta- tibiae each with a reduced barbulate anterior spur ("Ats" in Fig. 7E, H) and a well-developed pectinate posterior spur ("Pts" in Fig. E - F, H); posterior spurs with dense seta-like cuticular projections except

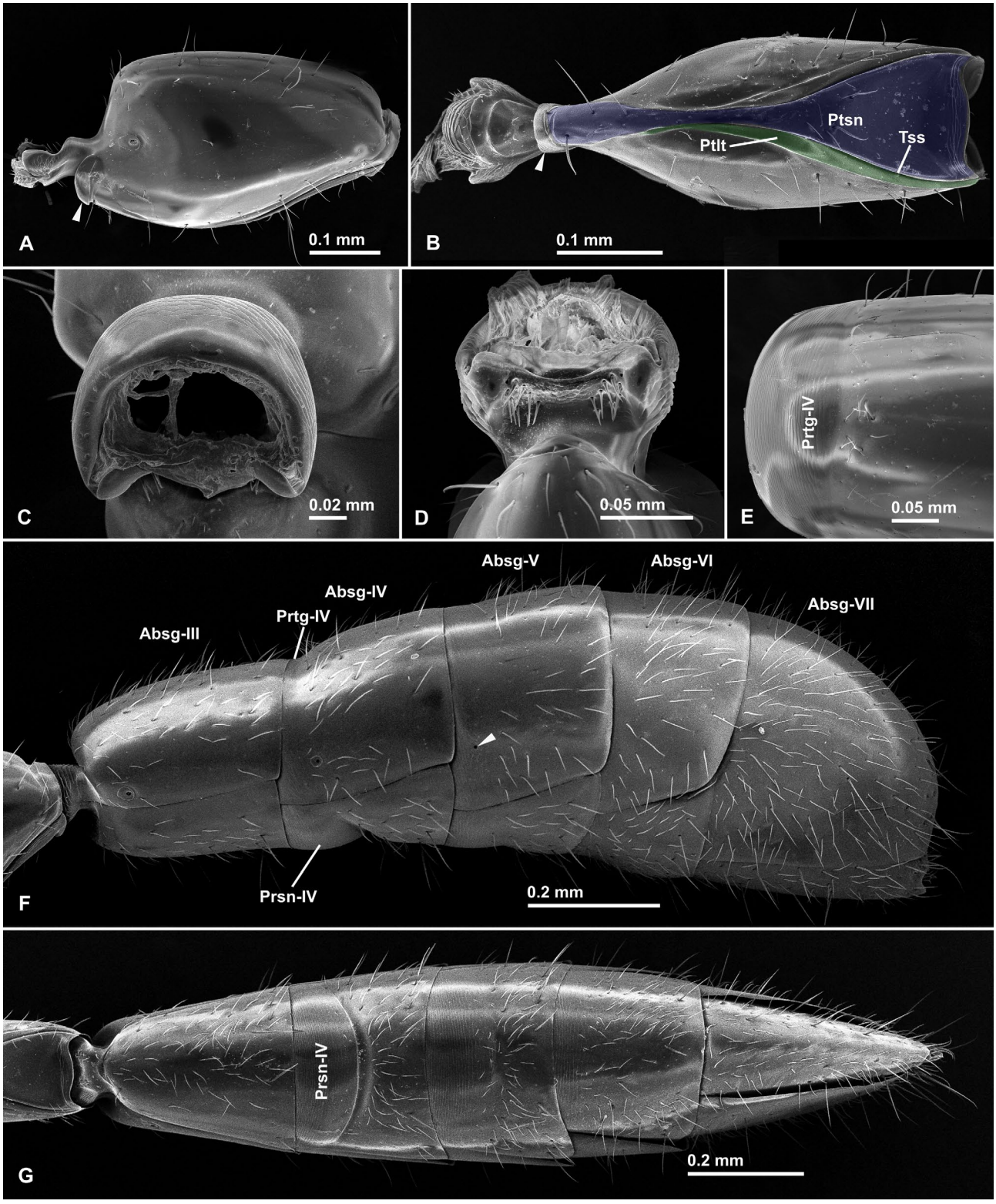


Fig. 8: Scanning electron microscope images of metasoma of *Opamyrma hungvuong* worker, nontype (AKY05vii17-06, China, Guangxi). (A) petiole in lateral view; (B) petiole in ventral view; (C) helcium in anterior view; (D) helcium in ventral view; (E) pretergite of abdominal segment IV in dorsal view; (F) gaster in lateral view; (G) gaster in ventral view. Abbreviations: Absg = abdominal segment; Prsn = presternite; Prtg = pretergite; Ptlt = petiolar laterotergite; Ptsn = petiolar sternite; Tss = tergosternal suture.

for basiposterior surface of the metatibial spur. Apically truncated and somewhat flattened setae present on posterior face of metatibia near insertion of the posterior spur; similar setae also present posterior face of metabasitarsus along its inner margin (arrows in Fig. 7F). Anterior surface of probasitarsal notch with numerous acute scale-like

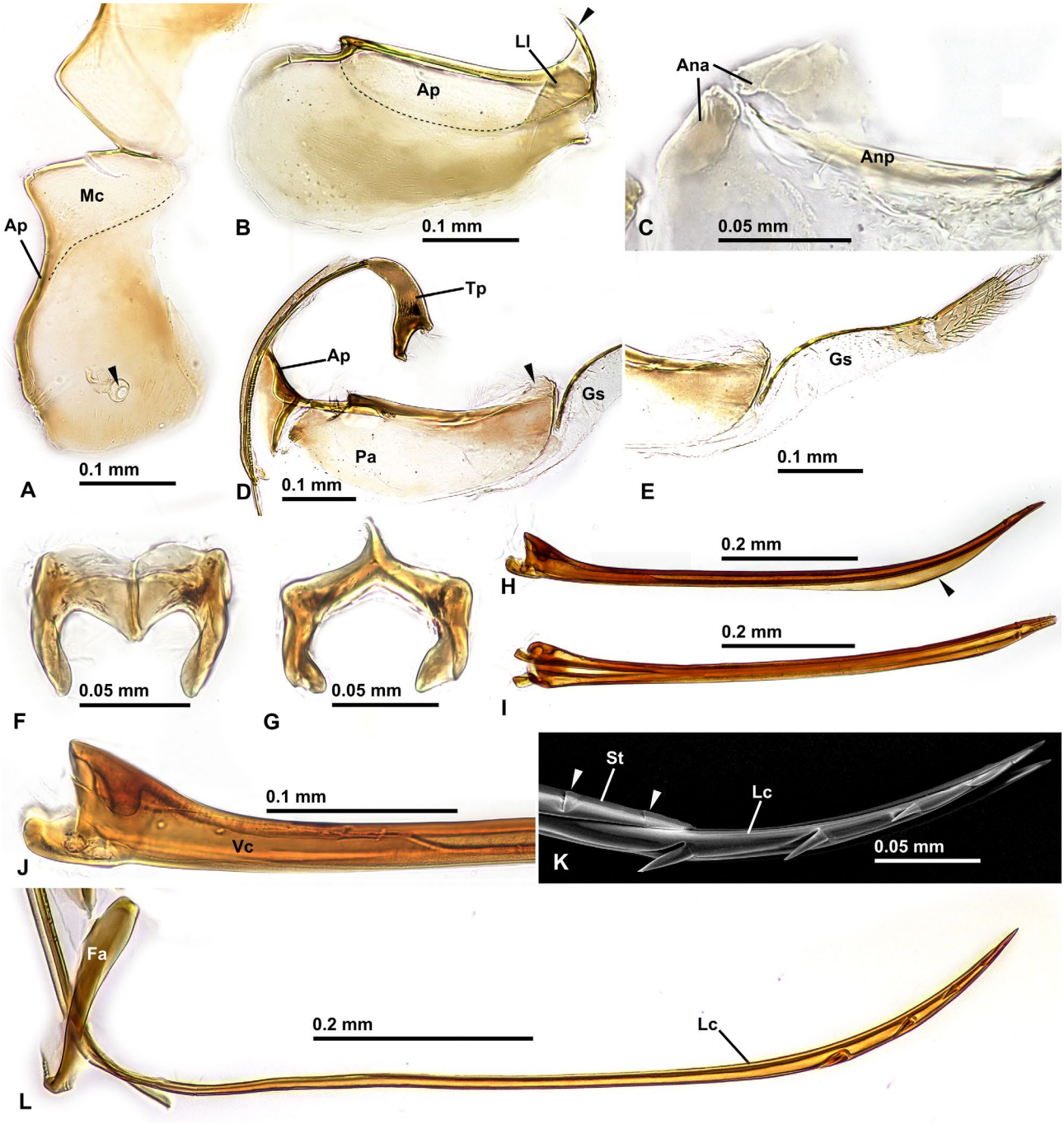


Fig. 9: Sting apparatus of *Opamyrma hungvuong* worker, nontype (AKY05vii17-06, China, Guangxi). (A) spiracular plate in lateral view; (B) quadrate plate in lateral view; (C) anal arcs and anal plate in flattened dorsal view; (D) oblong plate and triangular plate in lateral view; (E) gonostylus in lateral view; (F) furcula in anterodorsal view; (G) furcula in posterior view; (H) sting in lateral view; (I) sting in dorsal view; (J) basal part of sting in lateral view; (K) Scanning electron microscope image of apical parts of sting and lancet in lateral view; (L) lancet and fulcral arm in lateral view. Abbreviations: Ana = anal arc; Anp = anal plate; Ap = anterior apodeme; Fa = fulcral arm; Gs = gonostylus; Lc = lancet; Ll = lateral lobe; Mc = medial connection; Pa = posterior arm; St = sting; Tp = triangular plate; Vc = valve chamber.

cuticular projections (Fig. 7A - B); posterior surface of the probasitarsal notch without any stout spiniform seta (Fig. 7C). Anterior surfaces of distal portion of protibia and probasitarsus bearing numerous spatulate setae (Fig. 7A - B). Basiventral margin of probasitarsus just rounded, not strongly produced. Posteroventral corner of protarsomeres I - III respectively with some conspicuous stout spiniform setae (arrows in Fig. 7D). Stout spiniform setae absent on mesotibia, mesobasitarsus, and metabasitarsus (except for stout setae near distal margin of mesobasitarsus). Pretarsal manubrium ("Mnb" in Fig. 7G) relatively large, flat and longitudinal elliptical, with a pair of stout long setae (no

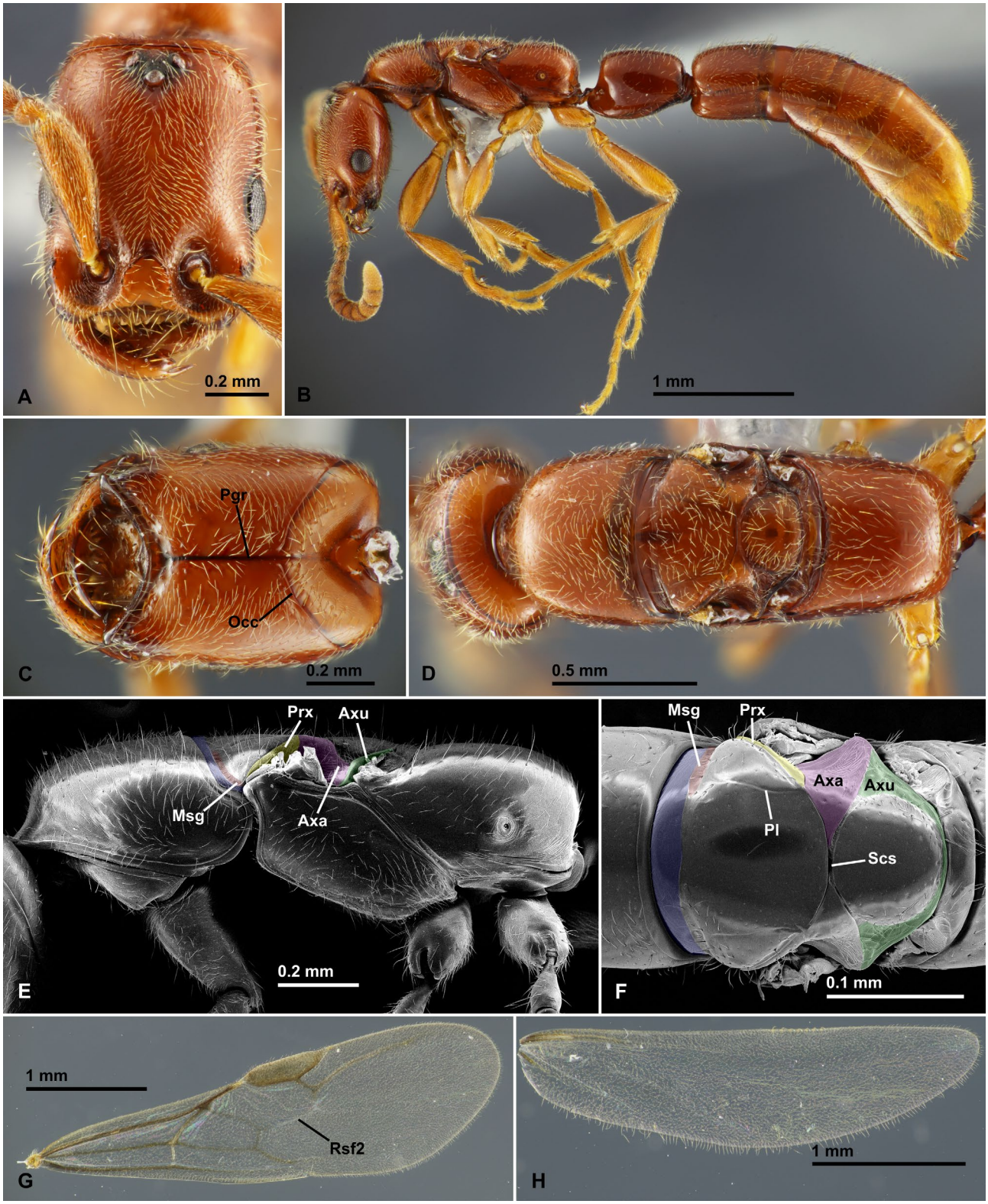


Fig. 10: *Opamyrma hungvuong* queen, nontype (Dai19iii2019-029, Son La, Vietnam). (A) head in full-face view; (B) body in lateral view; (C) head in ventral view; (D) head and mesosoma in dorsal view; (E) Scanning electron microscope image of mesosoma in lateral view; (F) Scanning electron microscope image (SEM) of meso- and metanotum in dorsal view; (G) forewing in dorsal view; (H) hindwing in dorsal view. Abbreviations: Axa = axilla; Axu = axillula; Msg = mesonotal groove; Occ = occipital carina; Pgr = postgenal ridge; Pl = parapsidal line; Prx = preaxilla; Rs = radial sector; Scs = scutoscutellar sulcus.

significant differences between those of pro-, meso- and meta legs). Pretarsal claws simple, without teeth (Fig. 7G).

Metasoma. Waist 1-segmented, that is, consisting of only petiole (abdominal segment II). Petiole subrectangular to oblong in lateral view, virtually sessile without distinct anterior peduncle, longer than wide in dorsal view, with slightly convex dorsal face that roundly continues to lateral face; petiolar sternite in ventral view ("Ptsn", marked by blue color in Fig. 8B) disproportionate dumbbell-shaped, with narrow elongated anterior part, only anteriorly fused with the tergite; posterior part of the sternite delimited from the tergite by distinct tergosternal suture ("Tss" in Fig. 8B); petiolar laterotergite ("Ptlt", marked by green color in Fig. 8B) present as narrow area along the tergosternal suture; petiolar spiracle located anteriorly on the lateral face of the tergite at its mid-height; anteroventral corner of petiole with flange-like structure (arrow in Fig. 8A - B); petiolar levator process complete, without lacuna; very short tubular posterior peduncle present inside which the helcium articulates. Gaster very elongate and laterally compressed especially in posterior segments, in lateral view highest at the posterior end of abdominal segment V. Helcium axial (sensu Keller 2011), tergosternally fused; helcium sternite laterally enclosed in the tergite. Postsclerites of abdominal segment III tergosternally unfused, having a free anterior face above the helcium, longer than high, narrowed basally in dorsal view, longer than segments IV, V and VI. Prora of abdominal sternite III present as a strong corner that is produced anteriad to reaching the level of the anteriormost point of tergite III. Abdominal spiracle III located on lower lateral face of the tergite. Abdominal segment IV with externally visible presclerites; pretergite ("Prtg-IV" in Fig. 8E - F) short and inconspicuous, just weakly constricted; presternite ("Prsn-IV" in Fig. 8F - G) long and conspicuous, posteriorly delimited by strong constriction. Abdominal spiracles IV - V visible, but VI - VII concealed by preceding tergites (the original description stated that spiracles V is concealed, but it is clearly visible as indicated by arrow in Fig. 8F). Abdominal segment VII longest among the segments III - VII. Pygidium (abdominal tergite VII) very large and simple, unarmed, convex and downcurved posteriorly in lateral view. Hypopygium (abdominal sternite VII) unarmed, in ventral view long subtriangular.

Sting apparatus. Lateral hemitergites of spiracular plate (abdominal tergite VIII) narrowly attached each other by large medial connection ("Mc" in Fig. 9A ); the attachment present as a suture-like, strongly sclerotized midline; median connection distinctly delimited from the main disc (= "body" sensu Kugler, 1978) by a weak carina (indicated by dashed line in Fig. 9A); main disc subrectangular with broadly concave posterodorsal margin, without distinct dorsal notch; spiracle (arrow in Fig. 9A) relatively large, located lower (ventrad) center of the disc; posteroventral corner without posterodorsal lobe and tubercle; anterior apodeme ("Ap" in Fig. 9A) narrow. Anterior apodeme ("Ap" in Fig. 9B) of quadrate plate (abdominal tergite IX) much smaller than its main disc, delimited by distinct midplate line (partially indicated by dashed line in Fig. 9B), with large lateral lobe ("Ll" in Fig. 9B); anterodorsal corner (arrow in Fig. 9B) long and sharp. Anal arcs and plate present ("Ana" and "Anp" in Fig. 9C), weakly sclerotized apparently without anal sensilla. Anterior apodeme ("Ap" in Fig. 9D) of oblong plate (gonocoxa IX; = second valvifer) forming small subtriangular sclerite in lateral view, that is posteriorly margined by diverging thickened ridge that is connected with dorsal ridge of the posterior arm ("Pa" in Fig. 9D); posterior arm relatively large, more than twice as long as high in lateral view: dorsal subterminal part of the arm (arrow in Fig. 9D) forming weakly sclerotized flange protruding from the dorsal ridge; most of ventral arm inconspicuous and apparently membranous; fulcral arm ("Fa" in Fig. 9L) large and linear. Basal part of triangular plate (gonangulum; = first valvifer; "Tp" in Fig. 9D) long and thin, weakly curved; lateral tubercle apparently absent; dorsoapical and ventroapical processes short and stout. Gonostylus (gonoplac; = third valvula; "Gs" in Fig. 9D, E) long and slender, composed of 2 distinct segments; first segment long and feebly sclerotized except for well-sclerotized dorsal margin, with sparse short erect setae along dorsal margin and on posterior part of its outer face; second segment short, relatively well-sclerotized, with denser and longer erect setae on its outer face. Furcula (Fig. 9F - G) thick, Y-shaped in posterior view, with short dorsal arm, unfused with sting base. Sting (gonapophysis IX; = stylet, second valvula; Fig. 9H - K) very narrow elongate and blade-like; sting bulb conspicuously wider and higher than base of the shaft; valve chamber ("Vc" in Fig. 9J) present but narrow; sting shaft more than twice as long as valve chamber, upcurved, with two pairs of small barbs on the apex (arrows at "St" in Fig. 9K); distiventral edge of the shaft produced to form broad lamina (arrow in Fig. 9H). Lancet (gonapophysis VIII; = first valvula; "Lc" in Fig. 9L) completely lacks valves, with 5 apical barbs of which basal three are conspicuously large and directed ventrad, and apical two are small and inconspicuous.

Color, sculpture, and pilosity. Body entirely light orangish brown, with slightly yellowish antennae and legs. Body largely smooth and shining. Body largely covered with sparse to dense decumbent / standing hairs as shown in figures: hairs most dense in dorsum of cranium, and most sparse in posterolateral face of mesonotum and lateral face of petiole; a series of particularly thicker and longer hairs present along anterior margin of cranium in full-face view.

**Queen (Fig. 10):** Fully winged, largely similar to the worker except for optic- and flight-related characters described below. Eyes and ocelli large and conspicuous; eyes circular with about 15 ommatidia at maximum diameter in lateral view, located a little lower of mid-length of cranium in full-face view; ocelli located high close to occipital carina. Occipital carina ("Occ" in Fig. 10C) nearly complete, but interrupted at midline of the venter. Postgenal ridge


Fig. 11: *Opamyrma hungvuong* male, nontype (Dai19iii2019-029, Son La, Vietnam). (A) head in full-face view; (B) head and mesosoma in lateral view; (C) mouthparts in anteroventral view; (D) head and mesosoma in dorsal view; (E) petiole in lateral view; (F) metasoma in lateral view; (G) petiole in ventral view; (H) metasoma in dorsal view. Abbreviations: Atp = anterior tentorial pit; Lbp = labial palp; Lbr = labrum; Mdl = mandalus; Mxp = maxillary palp; Nt = notauli; Pl = parapsidal line; Pv = penisvalva; Tm = telomere; Tsl = tergosternal line.

("Pgr" in Fig. 10C) extending more posteriorly, beyond the ventral interruption of occipital carina. Mesosoma having full complement of flight sclerites but still slender, with almost linear dorsal outline in lateral view; mesonotum not raised dorsally. Pronotum having large dorsal face as that of the worker. Dorsum of anterior articulatory area of mesonotum that inserted under the pronotum (marked by blue color in Fig. 10E - F) posteriorly delimited by a faint line and submedial weak narrow transverse grooves ("Msg", marked by red color in Fig. 10E - F) that is possibly homologous with that of the worker. Mesoscutum in dorsal view oval, much wider than long (excluding the anterior articulatory area); notauli absent; parapsidal lines ("Pl" in Fig. 10F) faintly present. Parascutal carinae weak. Preaxilla ("Prx", marked by yellow color in Fig. 10E - F) distinctly visible as narrow area in dorsal view. Axillae ("Axa", marked by purple color in Fig. 10E - F) in dorsal view large, strongly extending medially between mesoscutum and mesoscutellum but not meeting at midline. Axillulae ("Axu", marked by green color in Fig. 10E - F) large and conspicuous in dorsal view, virtually meeting each other behind mesoscutellum. Scutoscutellar sulcus ("Scs" in Fig. 10F) weak, very narrow and only faintly scrobiculate. Mesoscutellum in dorsal view circular, a little wider than long. Metascutellum large and conspicuous in dorsal view, not strongly produced in lateral view. Wing venation largely same as that of male (Fig. 10G - H, see also male description below), but Rsf2 faintly recognized as a vestigial spectral line in the queen forewing. Sting apparatus largely same as that of the worker.

**Male (Figs. 11 - 13):** C r a n i u m. In full-face view circular, almost as long as wide excluding eyes, with strongly convex posterior margin. Frontal carinae and lobes absent. Occipital carina absent. Eye and ocelli large and conspicuous; ocelli distantly located from eyes: median ocellus located just posterior to two-thirds of posterior part of cranium above eyes in full-face view. Antennal socket located in a large, roundly excavated area of which anterior wall is steep just behind the posterior margin of clypeus; the area not clearly defined posteriorly. Antennal torulus distinct, simple annular, distantly located from posterior clypeal margin (the distance slightly less than one torulus diameter). Anterior tentorial pit ("Atp" in Fig. 11A) situated anterior to antennal torulus. Median portion of the clypeus roundly raised dorsad; posterior area not inserted between antennal toruli, not quite reaching the level of anterior margin of the torulus; supraclypeal area distinct but indistinctly margined; lateral portion of clypeus in front of antennal socket narrow anteroposteriorly; median anterior clypeal margin weakly broadly concave, without any peg-like dentiform setae. Antenna 13-merous, filiform without becoming incrassate apically. Antennal scape short cylindrical, when laid backward, not reaching the level of posterior margin of eye in full-face view; antennomere II bead-like and shortest among antennomeres; antennomeres III–XII longer than wide, almost same length; antennomere XIII longest, with bluntly tapering apex. Mandibles strongly reduced, subtriangular nub-like, forming a broad gap when fully closed (Fig. 11A, C); masticatory margin edentate; mandalus ("Mdl" in Fig. 11A, C) large but still ringed by sclerite in dorsal view. Labrum ("Lbr" in Fig. 11C) subrectangular, more than twice as wide as long, with almost straight distal margin (median cleft absent); labral tuberculi absent; peg-like dentiform setae absent. Maxillary palp ("Mxp" in Fig. 11C) 4-segmented. Labial palp ("Lbp" in Fig. 11C) 2-segmented.

M e s o s o m a. Pronotum with conspicuously narrowed cervical shield; median pronotal area behind cervical shield convex and short in lateral view; maximum height of pronotum almost as long as mesoscutum height in lateral view. Mesoscutum large in dorsal view, much longer than wide; lateral margin concave around the anterior terminus of notauli. Notauli ("Nt" in Fig. 11D) distinct and weakly scrobiculate, meeting each other at the midline, but not extending to transscutal line (the posterior terminus located far from the transscutal line). Parapsidal line ("Pl", indicated by dashed line in Fig. 11D) present, weakly undulate. Parascutal carinae weak. Preaxilla distinctly visible as small area in dorsal view ("Prx" in Fig. 11D). Axillae small and conspicuous in dorsal view, moderately inserted between mesoscutum and mesoscutellum, not meeting each other at midline. Axillulae large and conspicuous in dorsal view, virtually meeting each other behind mesoscutellum. Scutoscutellar sulcus present as narrow and faintly scrobiculate groove, without crossribbing. Mesoscutellum in lateral view as high as mesoscutum, with convex dorsal margin, in dorsal view rounded subtrapezoidal, almost as long as wide. Metascutellum broad and conspicuously visible in dorsal view, in lateral view strongly produced. Mesopectus with oblique and weakly sinuate sulcus; anterior terminus of the sulcus located well ventral to pronotal corner. Metapleural spiracular plate absent. Anterior metapleural area weakly separated from posterior metapleural area by an inconspicuous transverse sulcus, and from propodeum by a deep conspicuous groove. Metapleural gland orifice occluded; internal structure of metapleural gland unrecognizable through metapleural sclerite. Propodeum in lateral view with roundly convex dorsal margin; posterior face roundly meeting dorsal and lateral faces without any delimiting carina; propodeal spiracle circular, large, low on lateral propodeal surface; propodeal lobe inconspicuous, just faintly developed. Metacoxal cavities fully closed with complete cuticular annuli surrounding the cavities, separated from propodeal foramen by a cuticular band.

M e t a s o m a. Waist 1-segmented, that is, consisting of only petiole (abdominal segment II). Petiole roundly swollen, virtually without distinct anterior peduncle, almost as long as wide and high, in lateral view with strongly convex dorsal margin; petiolar sternite unfused with the tergite, delimited by distinct tergosternal line ("Tsl" in Fig. 11E, G) even in anterior articulatory area; the sternite broad in ventral view, in lateral view with weakly convex ventral margin; subpetiolar process absent; petiolar laterotergite absent. Helcium axial (sensu Keller 2011), with sternite visible in lateral view, not enclosed by pretergite.

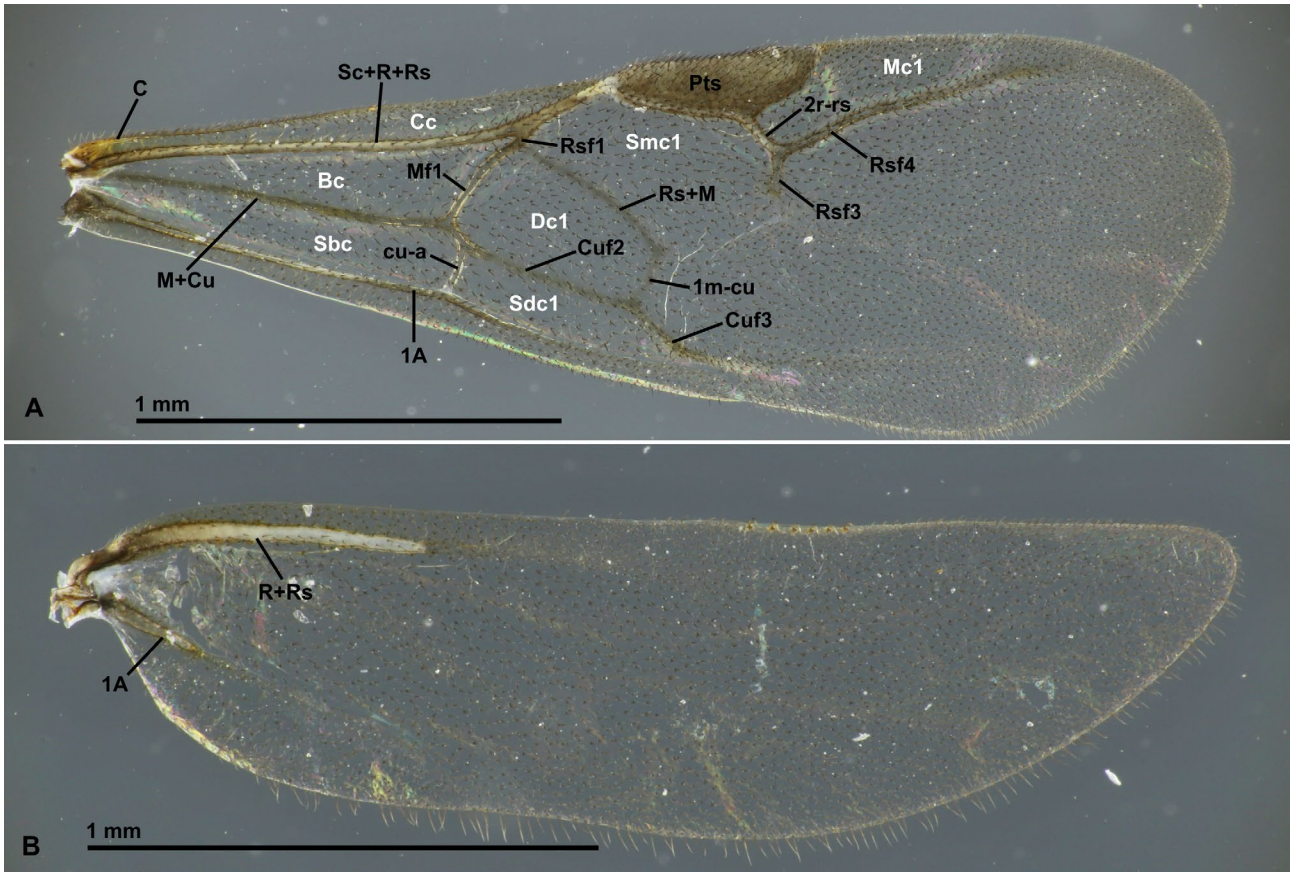


Fig. 12: Male wings of *Opamyrma hungvuong*, nontype (Dai19iii2019-029, Son La, Vietnam). (A) forewing in dorsal view; (B) hind wing in dorsal view. Abbreviations: 1A = first anal vein; Bc = basal cell; C = costal vein; Cc = costal cell; Cu = cubital vein; Mc1 = marginal cell 1; R = radial vein; Rs = radial sector; Sbc = subbasal cell; Sc = subcostal vein; Sdc1 = subdiscal cell 1; Smc = submarginal cell.

Abdominal postsclerites III tergosternally unfused. Prora of abdominal sternum III present just as weak carina delimiting poststernite from helcium; anteromedian area of helcium sternite concave. Abdominal tergites IV - VIII and abdominal sternites IV - IX well developed, not reduced or obscured. Abdominal segment IV without distinct presclerites. Abdominal spiracles III - V visible but VI - VIII concealed by preceding tergites. Abdominal segment IV longest among the segments III - VIII, a little longer than segments III and V. Abdominal tergite VIII unarmed.

Wings (Fig. 12). Wings hyaline, completely covered by fine setose layer. Forewing venation reduced with only three closed cells (basal, subbasal, and discal), categorized as Ogata's venation type IVb, although discal cell enclosed by nebulous Rs + M and 1 m-cu; pterostigma large and conspicuous; free R distal to pterostigma absent; costal vein (C) tubular only in short basal part and soon disappearing distally (costal cell open); Rsf1 tubular, very short and nearly lost; Mf1 tubular, completely closing basal cell; Rs + M nebulous; Rsf2 absent; Rsf3 only partially weakly present as a short diverging branch from Rsf4 (submarginal cell 1 unclosed); Rsf4 + tubular, continuous with 2r-rs which is directed posteroapically, ending before wing apex (marginal cell 1 open); Mf3 + absent and 2rs-m absent (submarginal cell 2 absent); 1 m-cu nebulous (discal cell 1 closed); M + Cu tubular (basal cell closed); Cuf2 - 3 nebulous; 1A tubular, disappearing distally after the connection with cu-a (subdiscal cell 1 open; subbasal cell closed). Hindwing venation reduced, only with tubular R + Rs and 1A, with six hamuli; R not reaching anterior wing margin; 1A short; claval region relatively developed, with rounded margin; jugal lobe absent.

Genitalia (Fig. 13). Genitalia large and extremely specialized; most part of telomere and apical part of penisvalvae visible in external lateral view, without distension or dissection (see Fig. 11F). Pygostyles absent. Basal disc of abdominal sternite IX (Fig. 13C) distinctly more than twice wider than long when excluding spiculum, with anterolateral corner just weakly produced; posterior lobe very narrow, about one sixth as wide as basal disc, distinctly longer than basal disc when excluding spiculum, with strongly convex posterior apex; spiculum ("Spc" in Fig. 13C) long and acute, nearly as long as basal disc. Cupula (Fig. 13D, "Cu" in Fig. 13B, E) reduced, non-annular, only present as short half arc-shaped ventral sclerite. Parameres highly fused with each other both dorsally and ventrally (therefore a complete annulus formed), and also with penisvalvae dorsally, that is, parameres and pe-

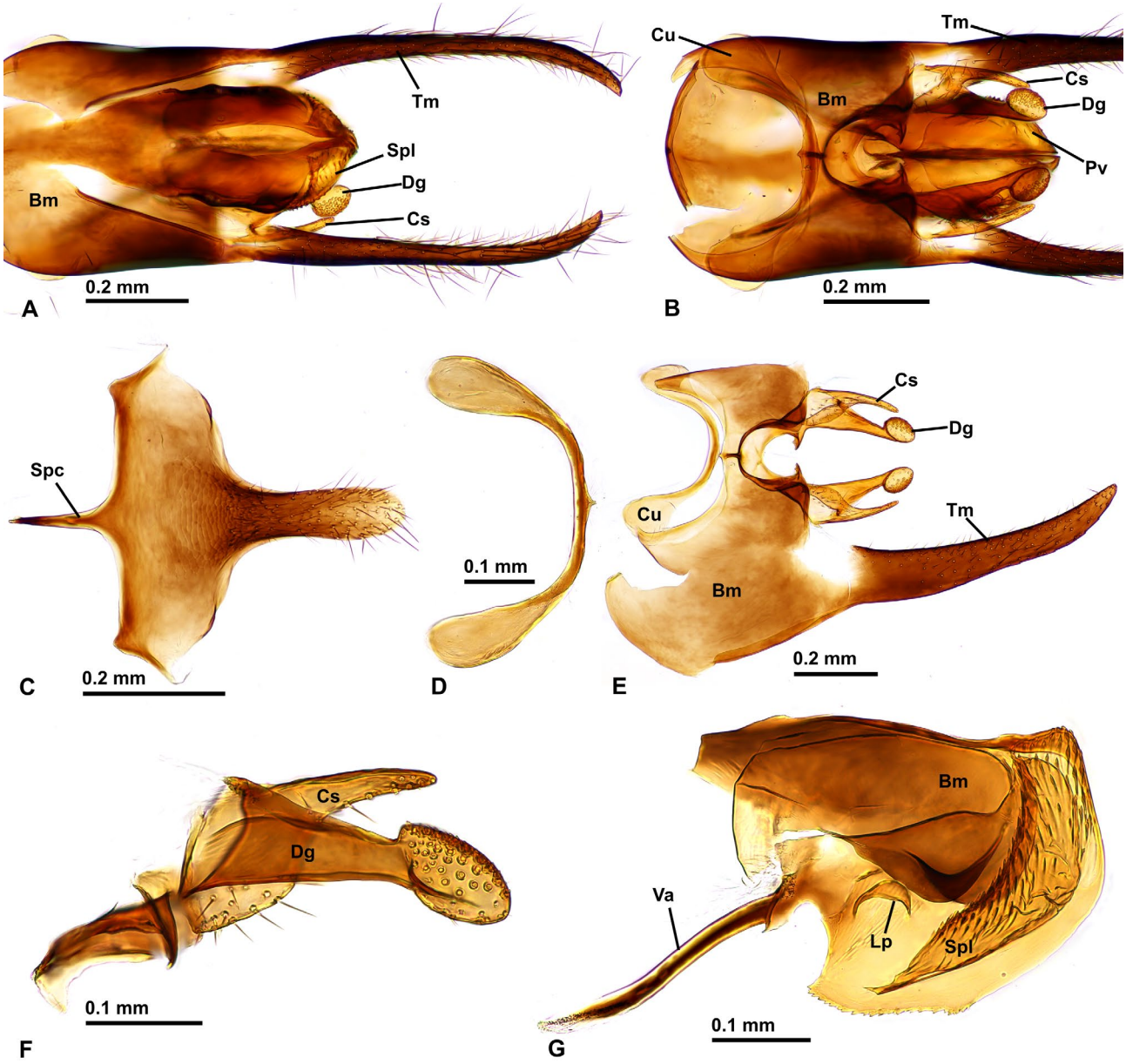


Fig. 13: Male genitalia of *Opamyrma hungvuong*, nontype (Dai19iii2019-029, Son La, Vietnam). (A) genital capsule in dorsal view; (B) genital capsule in ventral view; (C) abdominal sternite IX in ventral view; (D) cupula in ventral view; (E) left paramere with basiventral part of right paramere and cupula, in unfolded outer view; (F) left volsella in lateral view; (G) left penisvalva in lateral view. Abbreviations: Bm = basimere; Cu = cupula; Cs = cuspis; Dg = digitus; Lp = lateral apodeme; Pv = penisvalva; Spl = spinescent lobe; Spc = spiculum; Tm = telomere; Va = valvura.

nisvalvae inseparable without destruction (Fig. 13A - B); basivolsellae also strongly fused with each other ventrally and with basimeres; basimere ("Bm" in Fig. 13A - B, E, G) well-developed, without oblique carina on lower face ("BmC" sensu Yamada & Eguchi 2016); telomere ("Tm" in Fig. 13A, B, E) extremely elongate, distinctly longer than basimere, weakly recurved anteroventrad, clearly visible in external lateral view (see Fig. 11F), gently tapering apicad; articulation of basimere to telomere apparently fused, but differentiated by ventral membranous notch. Cuspis ("Cs" in Fig. 13A - B, E - F) distinct, elongate digitiform, with several short-modified setae on apical face and normal standing hairs on basal face. Digitus ("Dg" in Fig. 13A - B, E - F) club-shaped, with strongly swollen apical part directed laterad with numerous short modified setae on ventrolateral face. Penisvalvae (Fig. 13G, "Pv" in Fig. 13B) not fused with each other directly, but connected to each other via apical extension of basimere (dorsal sclerite apparently seem not be part of penisvalvae, but apical extension of basimere that extends lateroventrad and is fused partly with lateral face of valviceps; see Fig. 13G). Valvura ("Va" in Fig. 13G) elongate liner, directed anteroventrad. Valviceps with a modified lateral apodeme ("Lp" in Fig. 13G) that is visible as small semielliptic sclerite on

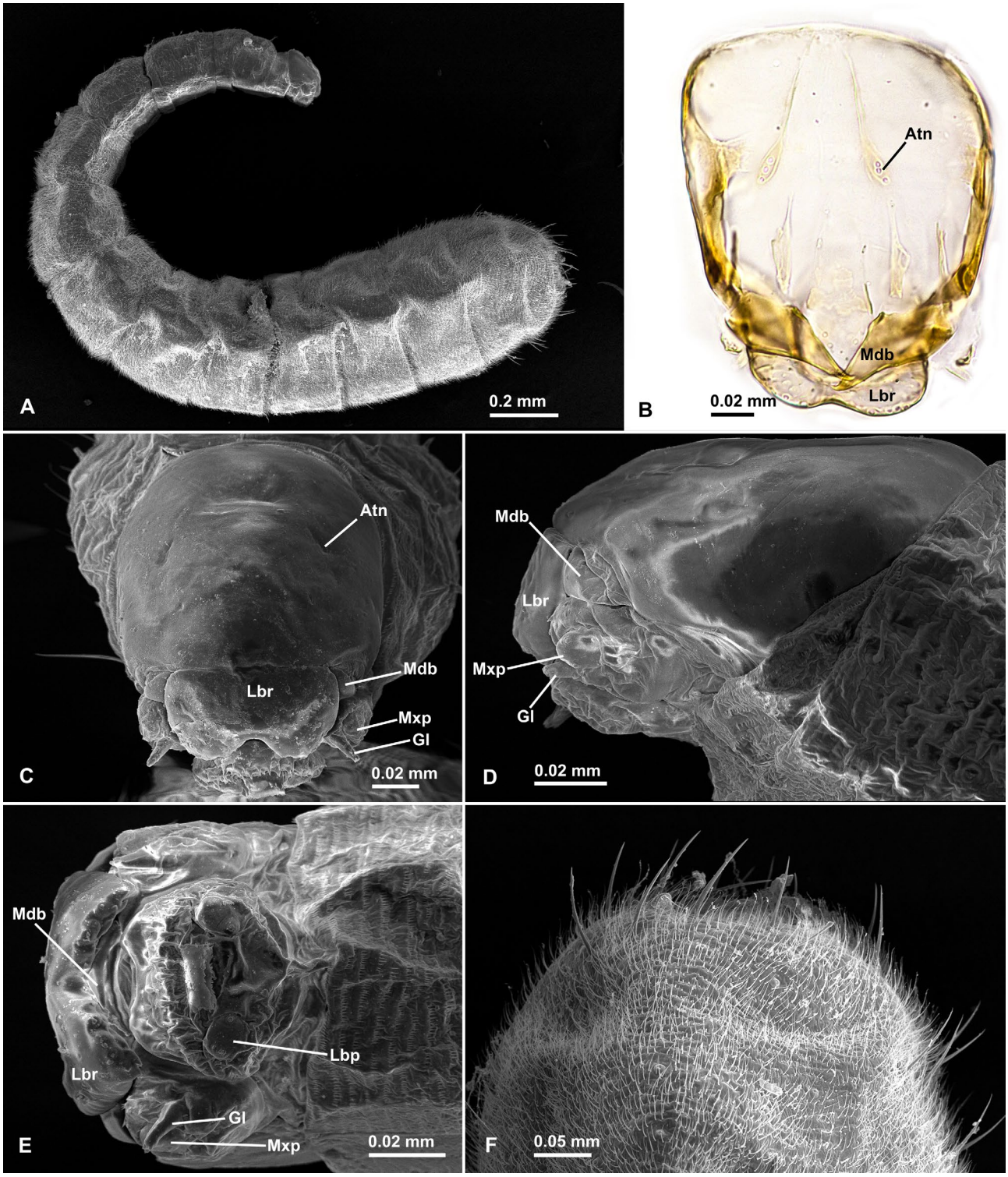


Fig. 14: Larva of *Opamyrma hungvuong*, nontype (AKY05vii17-06, China, Guangxi). (A) Scanning electron microscope (SEM) image of body in lateral view; (B) transmitted light microscopy image of head in dorsal view; (C) SEM image of head in frontal view; (D) SEM image of head in lateral view; (E) SEM image of head in ventral view; (F) SEM image of abdominal terminus in lateral view. Abbreviations: Atn = antenna; Gl = galea; Lbp = labial palp; Lbr = labrum; Mdb = mandible; Mxp = maxillary palp.

mid-height of basal valviceps in lateral view. Valviceps also have a uniquely specialized structure termed here as "spinescent lobe" ("Spl" in Fig. 13A, G); spinescent lobe originated from dorsoapical corner of the valviceps and extended ventrolaterally to form arc-shaped sclerite bearing numerous spines (therefore, it seems to be derived by extreme modification and sclerotization of penis-valvar membrane that commonly has numerous spines). Anteroventral corner of valviceps strongly produced with acute angle. Anterior part of ventral margin of valviceps

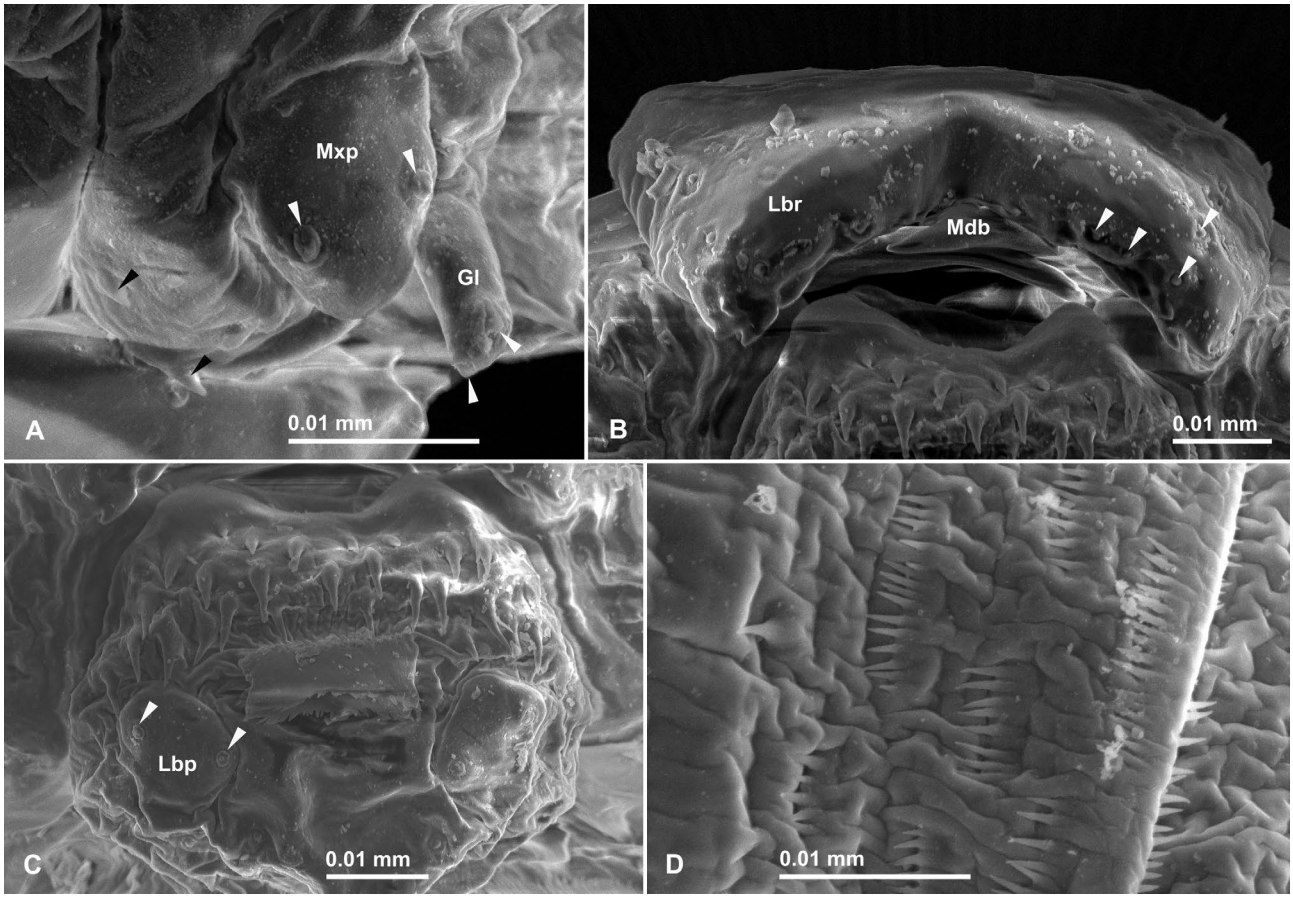


Fig. 15: Scanning electron microscope images of larval mouthparts and prothoracic surface of *Opamyrma hungvuong*, nontype (AKY05vii17-06, China, Guangxi). (A) left maxilla in dorsal view; (B) labrum in ventral view; (C) labium in ventral view; (D) cuticular spinules on prothorax. Abbreviations: Gl = galea; Lbp = labial palp; Lbr = labrum; Mdb = mandible; Mxp = maxillary palp.

with about 25 small teeth. Apical margin of valviceps rounded.

Color, sculpture, and pilosity. Body entirely black, with faintly paler antennae and legs; maxilla and labium whitish; telomere black; penisvalvae yellowish. Body largely smooth and shining. Body largely covered with sparse to dense decumbent / standing hairs as shown in figures; hairs most dense in dorsum of cranium, and sparser in mesosoma and metasoma.

**Larva (Figs. 14 - 15):** Following description is based on relatively developed larvae whose instar is unknown (with head width around 0.11 mm). Body elongate and slender with proportionally small head. Cranium longitudinally oval in full-face view, with smooth and hairless surface; posteromedian part just behind the level of antennae strongly depressed. Antenna ("Atn" in Fig. 14B - C) consisting of three sensilla located at the anterior end of a sulcus which extends from posterior end of cranium (the "sulcus" well-recognized as internal ridge in Fig. 14B). Mandible ("Mdb" in Fig. 14B - E) well-sclerotized, in dorsal view mostly concealed under labrum in the closed position, in dorsal view subtriangular with acute apex curved medially; masticatory margin linear and edentate. Maxilla with some cuticular spinules (black arrows in Fig. 15A); maxillary palp ("Mxp" in Fig. 14C - E, Fig. 15A) stout with two basiconic sensilla (white arrows on "Mxp" in Fig. 15A); galea ("Gl" in Fig. 14C - E) slender and digitiform with two basiconic sensilla (white arrows on "Gl" in Fig. 15A) on the apex. Labrum ("Lbr" in Fig. 14B - E) broad with anterior margin strongly and narrowly concave medially; surface near the anteroventral border with several basiconic sensilla (arrows in Fig. 15B). Labium with dense cuticular spinules on anteroventral surface; anterior margin in ventral view weakly broadly concave medially; labial palp stout, with two basiconic sensilla (arrows in Fig. 15C). Anteroventral surface of prothorax with dense transverse series of tiny cuticular spinules (Figs. 14E, 15D). Body hairs unbranched, with two types: 1) short thin standing hairs that very densely cover abdominal segments and sparsely present in thoracic segments; 2) stout standing hairs that very sparsely present in thoracic and abdominal segments, and especially numerous in around abdominal terminus (see Fig. 14F). Specialized structures such as "prothoracic projection" and "hemolymph tap" known in the *Leptanilla* larva absent. Spiracles unrecognizable in our observation (probably tiny and inconspicuous, as in the genus *Leptanilla*).

**Distribution:** This species has been recorded from southern area of China (Hainan, Guangxi) and northern central to northern Vietnam (Ha Tinh and Son La). Re-

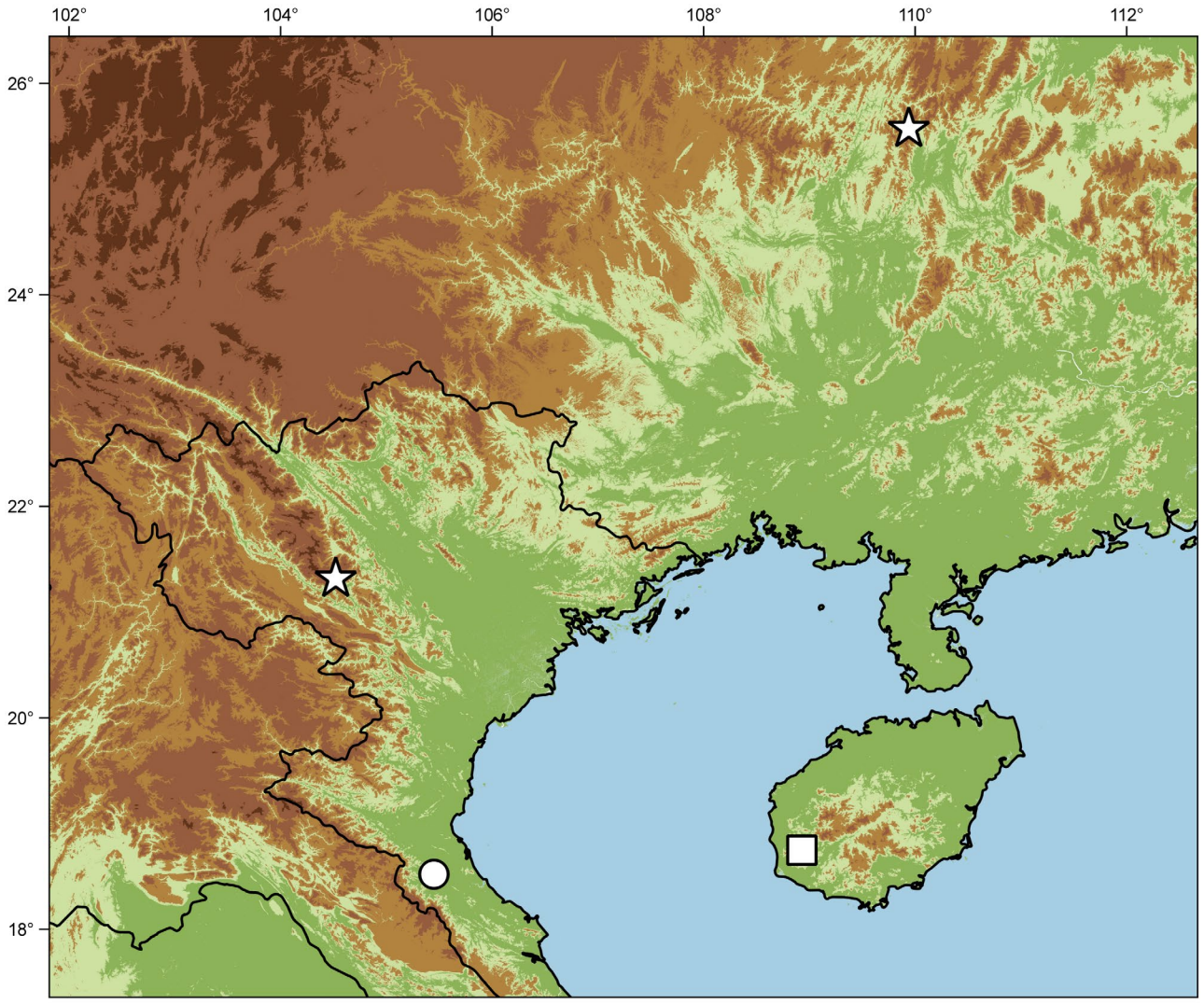


Fig. 16: Distribution map of *Opamyrma hungvuong*. Type locality, record by Chen & al. (2017), and new records by the preset study are indicated by circle, square, and stars, respectively.

corded elevations ranges from ca. 640 m a.s.l (in Hainan) to ca. 1500 m a.s.l (in Son La); the elevation of the type locality was not recorded. The confirmed distributional records are mapped in Fig. 16.

**Bionomics:** There are little data on the biology. Both of the two colonies examined in the present study were collected from soil on forest floor. The workers run agilely but didn't climb up smooth plastic walls. All 12 of the larvae from colony AKY05vii17-06 were approximately the same size, suggestive of brood cycles.

## Discussion

We here highlight the distinctive morphological characteristics of *Opamyrma* by comparison with other ant lineages, particularly other leptanilline genera, the apomyrmine genus *Apomyrma*, and the martialine genus *Martialis*.

**Female morphology:** The head of female *Opamyrma* is characterized by an occipital carina which is located well before the posterior margin of cranium in full-face view, and is complete and uninterrupted (in the worker) or is almost complete with a short medioventral interruption (in the queen). To our knowledge, such anterior location of occipital carina (and accompanying anterior extension of occiput) is unknown from any other extant or extinct ant lineage, and thus likely be an autapomorphy of *Opamyrma*. The location of the anterior invagination of tentorium in *Opamyrma* is also unusual. The anterior tentorial arm is invaginating from the anterior tentorial pit that is usually externally visible. The pits are located anteriorly on the dorsal surface of the cranium, at or very close to the posterior clypeal margin, and usually close to the antennal socket (from glossary in Fisher & Bolton 2016). However, in *Opamyrma*, the anterior tentorial pits are not externally visible, and apparently located on medioventral wall of antennal socket. Because ant tentoria have been very poorly studied (Kubota & al. 2019, Richter & al. 2019), future comprehensive studies on ant tentoria are needed to understand the morphological significance of the state observed in *Opamyrma*.

While female *Opamyrma* and *Apomyrma* have similarly shaped mandibles and numerous peg-like setae on the labrum, the present study highlights following differences between their mouthparts which were previously overlooked: 1) *Opamyrma* with single peg-like seta on ventral (internal) mandibular surface (absent in *Apomyrma*; see SEM images on AntWeb: ANTWEB1008505); 2) with mouthparts closed, the labrum of *Opamyrma* entirely conceals the prementum and maxillary stipes (reminiscent of the condition in the Dorylinae, see Borowiec 2016), whereas both prementum and maxillary stipes exposed in *Apomyrma*; 3) palp formula 4,2 in *Opamyrma*, 2,2 in *Apomyrma*.

Peg-like setae on the mouthparts and / or clypeus are particularly interesting, as they are present in the *Apomyrma*, some Leptanillinae (including *Opamyrma*), some Amblyoponinae, and, moreover, in Cretaceous stem-group genera (e.g., †*Gerontoformica*, †*Haidomyrmex* Dlussky, 1996, and †*Zigrasimecia* Barden & Grimaldi, 2013; see Barden & Grimaldi 2013, 2016). Besides *Opamyrma* and *Apomyrma*, a few to several labral peg-like setae are seen in the leptanilline genera *Protanilla* and *Anomalomyrma* Taylor, 1990, and the amblyoponine genera *Amblyopone* Erichson, 1842, and *Onychomyrmex* Emery, 1895 (see Borowiec & al. 2011, Yoshimura & Fisher 2014, Man & al. 2017, Hsu & al. 2017); *Protanilla* also have similar setae numerously along the masticatory margin of the mandible. Many amblyoponine genera (e.g., *Stigmatomma* Roger, 1859, *Amblyopone*, *Onychomyrmex*) also have peg-like setae on anterior margin of clypeus. The function of these peg-like setae has been proposed as a structure to grip active prey (Brown 1960, Yoshimura & Fisher 2014). Thus, the similarities of mandibular and labral morphology between *Opamyrma* and *Apomyrma* are likely associated with similar adaptation to handle active and soft-bodied prey such as geophilomorph centipedes, which has been suggested to be the primarily prey in *Apomyrma*, *Protanilla*, *Leptanilla*, and also some amblyoponines (Brown & al. 1971, Masuko 1990, 1993, Hsu & al. 2017). Nevertheless, it is currently uncertain whether the presence of these peg-like setae is a homoplastic trait within crown-group ants or a plesiomorphic trait of crown-group ants (because of its presence in some stem-group ants). Another notable morphological trait of the mouthparts that is seen in both *Apomyrma* and *Opamyrma* is the presence of long apically spatulate setae on the ventral face of the mandibles and the outer face of the labrum (for *Apomyrma*, see SEM images on AntWeb: ANTWEB1008505). The function of these unusual setae is a mystery.

The mesosoma of the worker of *Opamyrma* is similar to that of other leptanillines in having a metapleural longitudinal flange projecting laterad which overhangs (but does not conceal) the metapleural gland orifice, in agreement with the statement in the original description. This condition is one of the homoplastic synapomorphies of the subfamily Leptanillinae, and also appear in the subfamilies Pseudomyrmecinae and Heteroponerinae (Baroni Urbani & al. 1992, Bolton 2003, Keller 2011, Liu & al. 2019). The metasoma of female *Opamyrma* apparently exhibits plesiomorphic characteristics in the leptanillines that makes the habitus more similar to that of *Apomyrma* than that of other leptanillines: 1) tergosternal fusion of petiole absent posteriorly; 2) abdominal segment III not forming distinct postpetiole; 3) abdominal segment III unfused with petiole (the fusion seen exclusively in *Anomalomyrma*); 4) postsclerites of abdominal segment III tergosternally unfused; 5) presclerites of abdominal segment IV just weakly differentiated (especially pretergite).

The sting apparatus of *Opamyrma* is well-developed and apparently fully functional. In the aculeate Hymenoptera, two major types of venom ejecting mechanism are known, the valve-pump type and injection type (Van Marle & Piek 1986). In the valve-pump type, venom is ejected by shuttle movement of the lancets (= first valvulae) which possess valvular lobes (lancet valves) that act as pistons for pumping venom. In the injection type, venom is ejected by compression of a musculated venom reservoir. Among non-formicid aculeates, the valve-pump type is present in Apoidea, and the injection type in Vespidae and Pompilidae (Van Marle & Piek 1986, Kumpanenko & Gladun 2018). In ants, most stinging species are valve-pump type (Hermann 1969, Kugler 1978, Hermann & Blum 1981).

Despite the general pattern among ants, leptanillines likely have the injection type of venom ejection. Kugler (1992) described sting apparati of *Apomyrma*, *Leptanilla* and *Protanilla*, and suggested two apomorphies shared by the latter two leptanillines: 1) triangular plate with a lateral tubercle; 2) lancet valves and corresponding sting valve chamber absent. The loss of lancet valves suggests the use of an injection type mechanism. Indeed, an unusually large and massively musculated venom reservoir was reported in these two leptanilline genera (Hölldobler & al. 1989, Billen & al. 2013; their stinging acts on prey were reported in Masuko 1990, Hsu & al. 2017). The present study revealed that the sting apparatus of *Opamyrma* exhibits a mosaic of plesiomorphic and apomorphic traits: 1) triangular plate apparently without a lateral tubercle; 2) lancet valves absent but small sting valve chamber present. Thus, it is likely that *Opamyrma* also use the injection type mechanism. Considering that both the lancet valves and valve chamber are present in *Martialis* (see Brandão & al. 2010), the loss of the lancet valves in the fully functional sting apparatus and accompanying shift to injection type may be a non-homoplastic synapomorphy of the subfamily Leptanillinae (within the Formicidae), although the sting apparatus of *Anomalomyrma* has yet to be described. The loss of the valve chamber may have evolved later in the derived lineages, for example, *Protanilla* and *Leptanilla*. The injection type may facilitate rapid ejection of venom and help hunting relatively large active prey. Although the loss of lancet valves itself was also reported in the doryline genus *Dorylus* Fabricius, 1793 and myrmicine genus *Atta* Fabricius, 1804, their sting apparati are reduced and not functional for stinging (Hermann 1969, Hermann & al. 1970). Furthermore, the leptanillines share relatively large

barbs on the sting and lancets that can provide a firm grip on active prey. It is also notable that the leptanillines have an unfused furcula, which is a small but functionally important component for sting maneuverability (Hermann & Chao 1983). In ants, according to Hermann & Chao (1983), the fusion of furcula with sting base occurs in the dolichoderines, aneuretines, dorylines, at least one ponerine (in the genus *Simopelta* Mann, 1922), and possibly some myrmicines.

Future comprehensive studies of ant sting apparati and exocrine systems are necessary for further developing our understanding of the evolution of sting apparatus morphology and venom ejecting mechanisms. It is also worth comparing functional morphology and hunting behavior between *Opamyrma* and *Apomyrma*, which share similar head and metasoma morphology (and possibly similar prey) as mentioned above, while having different venom ejecting mechanisms.

The queen of *Opamyrma* is fully winged but has a slender mesosoma, together with undifferentiated morphology of mandibles, and sting apparatus from those of the workers. Although we have no direct data on life history of *Opamyrma* (and also most other leptanillines), the morphological characteristics of the *Opamyrma* queen are suggestive of non-claustral independent colony founding in which queens need to forage outside the nest. Collection of a dealate queen with a single worker by Chen & al. (2017) is also suggestive of this. The injection type of venom ejection may also help solitary hunting by queens. Interestingly, in *Leptanilla* that are considered to reproduce by obligate dependent colony foundation with specialized ergatoid queens (Masuko 1990), the sting apparatus morphology is unusually highly differentiated between the worker and queen (Kugler 1992). The presence / absence of caste dimorphism in sting apparatus morphology is unknown in *Protanilla*, in which both alate and ergatoid queens have been reported (Billen & al. 2013, Hsu & al. 2017).

**Male morphology:** The male of *Opamyrma* is similar to other known leptanilline males in sharing the following derived characters: reduced nub-like mandibles, reduced wing venation (Ogata's venation type IVb), inconspicuous propodeal lobes, and extremely derived genitalia with reduced cupula (Petersen 1968, Ogata & al. 1995, Boudinot 2015). *Opamyrma* males can also be identified as a leptanilline based on the male-based key by Boudinot (2015), with minor deviations. That key noted that leptanilline males have "at most only three closed cells (costal, basal, subbasal)" in the forewing. However, in *Opamyrma*, in addition to basal and subbasal cells, the discal cell is also closed by the presence of weak inconspicuous Rs + M, 1 m-cu, and Cuf2. Based on Boudinot (2015), following reduction of forewing venation of *Opamyrma* shows affinity between *Opamyrma* and other leptanillines: 1) Rsf1 virtually lost (present in *Apomyrma*); 2) loss of free R distal to the pterostigma (present in *Apomyrma*); 3) Rs + M non-tubular / absent (tubular in *Apomyrma*); 4) Mf2 + non-tubular / absence (free M after Rs + M; tubular in *Apomyrma*); 5) 1 m-cu non-tubular and nebulous (tubular in *Apomyrma*; absent in *Martialis*, Leptanillini, Anomalomyrmini). Nevertheless, the *Opamyrma* male is clearly differentiated from the other leptanilline males (including four genera known only from males, namely *Noonilla* Petersen, 1968, *Phaulomyrma* Wheeler & Wheeler, 1930, *Scyphodon* Brues, 1925, and *Yavnella* Kugler J, 1987) by the absence of tergosternal fusion in the petiole which is likely a plesiomorphic character in leptanillines.

The male genitalia of *Opamyrma* are extremely derived in having: 1) reduced non-annular cupula, only present as short half arc-shaped ventral sclerite; 2) basimeres bilaterally fused dorsally and ventrally, and with apical extension that extends lateroventrad and is fused with lateral face of valviceps; 3) extremely elongate telomeres, largely visible in external view and directed anteroventrad; 4) modified lateral apodeme and "spinescent lobe" of valviceps.

The reduction of cupula is also seen in other leptanillines and some non-leptanillines (e.g., some dolichoderines (see Barden & al. 2017), some dorylines (see Borowiec 2016), and myrmicine genus *Anillomyrma* Emery, 1913 (see Yamane & Jaitrong 2019)), but the condition of *Opamyrma* is unique in that cupula has modified to be a just small ventral sclerite. In the *Leptanilla* the reduced cupula apparently fused with sternite IX (Petersen 1968, Ogata & al. 1995). Thus, the cupular condition of *Opamyrma* seems to be relatively plesiomorphic in leptanillines in terms of presence of unfused cupula, although the cupular condition in the other leptanillines is currently unclear (Boudinot 2015).

The dorsomedial fusion between the basimere and penisvalvae are similar to the condition in *Apomyrma* CD01 (see Boudinot 2015). However, the homology of the dorsal sclerite of the penisvalvae between the *Opamyrma* and *Apomyrma* seems to be doubtful. In *Opamyrma*, the penisvalvae seem to be connected indirectly with each other via apically extended basimere, whereas in the *Apomyrma*, the penisvalvae are fused directly with each other. To our knowledge, the structure similar to the "spinescent lobe" in *Opamyma* has never been described in other ant lineages. This unique structure is apparently derived by extreme modification and sclerotization of the penisvalva membrane, which commonly has numerous spines. The spines of the "spinescent lobe" may potentially damage female genitalia during copulation, that is, possibly cause traumatic mating (Lange & al. 2013). Although the mating behavior of leptanillines including *Opamyrma* is entirely unknown, the general tendency of extreme and diverse specialization of male genitalia in leptanillines suggests that they may have inherited common biological properties that reinforces sexual selection on male genital morphology from their most recent common ancestor (the male genitalia are less specialized in putative *Martialis* males, see Boudinot 2015).

**Larval morphology:** In leptanillines, detailed description of the larva is available only in *Leptanilla*. The larvae of *Leptanilla* are highly specialized in having the following characters related to larval hemolymph feeding (LHF, regular feeding on the hemolymph of their

own larvae by adults), nomadism, and specialized predation of geophilomorph centipedes: 1) outwardly directed mandibles, which help the larva to sink their head into the centipede body; 2) the "prothoracic projection" used for larval transportation by workers; 3) the "hemolymph tap", which is a specialized organ for LHF (Wheeler & Wheeler 1965, 1989, Masuko 1989, 1990, 2008, Barandica & al. 1994). The larva of *Opamyrma* lacks all of these specialized characters, whereas it retains some similarity with *Leptanilla* larvae: 1) slender and elongated body with small hairless cranium; 2) spiracles tiny and inconspicuous (invisible in the present study); 3) body hairs simple, with dense short hairs and sparse long stout hairs. Thus, the *Opamyrma* larva seems to retain the most plesiomorphic characters among the members of the subfamily Leptanillinae. LHF has been observed in twelve ant genera from five subfamilies, but the "hemolymph tap" is known only in *Leptanilla* and the proceratiine genus *Proceratium* Roger, 1863 (see Masuko 2019). In the other genera that perform LHF but do not have a specialized organ for it (e.g., *Stigmatomma*, see Masuko 1986), the queen and worker bite larva non-lethally and imbibe the hemolymph leaking from the wound. Future behavioral study of *Opamyrma* colonies are needed to confirm the presence / absence of LHF. Data on larvae of other leptanilline genera and *Martialis* are also necessary for further understanding the evolution of larval morphology.

**Conclusion:** The present study supports the phylogenetic position of the genus *Opamyrma* as the most basal lineage in the subfamily Leptanillinae, as supported by recent phylogenetic analyses (Ward & Fisher 2016, Borowiec & al. 2019), by providing novel knowledge on the morphology of this extremely rare genus. The loss of lancet valves in the fully functional sting apparatus with an accompanying shift to the injection type of venom ejecting mechanism is suggested as a potential non-homoplastic synapomorphy of this subfamily within the Formicidae. On the other hand, *Opamyrma* retains plesiomorphic traits not seen in the other leptanillines, such as the presence of sting's valve chamber, absence of tergosternal fusion in petiole (excluding its anterior part in female), absence of postpetiolation, and less-specialized larval morphology.

**Acknowledgments**

We would like to thank Shanyi Zhou (Professor Emeritus, Guangxi Normal University (GXNU), China), Zhi-lin Chen (GXNU), Nguyen Van Sinh (Director, Institute of Ecology and Biological Resources (IEBR), Vietnam), Truong Xuan Lam (Vice Director, IEBR), Nguyen Duc Anh (IEBR), and the directors and staffs of Huaping National Nature Reserve (Guangxi, China) and Ta Xua Nature Reserve (Son La, Vietnam), for their help in the field surveys; Adam L. Cronin (Tokyo Metropolitan University, Japan) for help in making linguistic corrections on the final draft; Brendon E. Boudinot and Marek L. Borowiec for their valuable comments. The second author, Nguyen Dac Dai, is supported by the Japanese Government (Monbukagakusho: MEXT) Scholarship. Research activity of the last author, Katsuyuki Eguchi, was supported by Asahi Glass Foundation (Leader: Katsuyuki Eguchi; FY2017–FY2020).

**References**

Barandica, J.M., López, F., Martínez, M.D. & Ortuño, V.M. 1994: The larvae of *Leptanilla charonea* and *Leptanilla zaballosi*. – Deutsche Entomologische Zeitschrift 41: 147-153.

Barden, P., Boudinot, B. & Lucky, A. 2017: Where fossils dare and males matter: Combined morphological and molecular analysis untangles the evolutionary history of the spider ant genus *Leptomyrmex* Mayr (Hymenoptera: Dolichoderinae). – Invertebrate Systematics 31: 765-780.

Barden, P. & Grimaldi, D. 2013: A new genus of highly specialized ants in Cretaceous Burmese Amber (Hymenoptera: Formicidae). – Zootaxa 3681: 405-412.

Barden, P. & Grimaldi, D. 2016: Adaptive radiation in socially advanced stem-group ants from the Cretaceous. – Current Biology 26: 515-521.

Baroni Urbani, C., Bolton, B. & Ward, P.S. 1992: The internal phylogeny of ants (Hymenoptera: Formicidae). – Systematic Entomology 17: 301-329.

Billen, J., Bauweleers, E., Hashim, R. & Ito, F. 2013: Survey of the exocrine system in *Protanilla wallacei* (Hymenoptera: Formicidae). – Arthropod Structure & Development 42: 173-183.

Bolton, B. 2003: Synopsis and classification of Formicidae. – Memoirs of the American Entomological Institute 71: 370 pp.

Borowiec, M.L. 2016: Generic revision of the ant subfamily Dorylinae (Hymenoptera, Formicidae). – ZooKeys 608: 1-280.

Borowiec, M.L., Rabeling, C., Brady, S.G., Fisher, B.L., Schultz, T.R. & Ward, P.S. 2019: Compositional heterogeneity and outgroup choice influence the internal phylogeny of the ants. – Molecular Phylogenetics and Evolution 134: 111-121.

Borowiec, M.L., Schulz, A., Alpert, G.D. & Baňař, P. 2011: Discovery of the worker caste and descriptions of two new species of *Anomalomyrma* (Hymenoptera: Formicidae: Leptanillinae) with unique abdominal morphology. – Zootaxa 2810: 1-14.

Boudinot, B.E. 2013: The male genitalia of ants: musculature, homology, and functional morphology (Hymenoptera, Aculeata, Formicidae). – Journal of Hymenoptera Research 30: 29-49.

Boudinot, B.E. 2015: Contributions to the knowledge of Formicidae (Hymenoptera, Aculeata): a new diagnosis of the family, the first global male-based key to subfamilies, and a treatment of early branching lineages. – European Journal of Taxonomy 120: 1-62.

Boudinot, B.E., Sumnicht, T.P. & Adams, R.M.M. 2013: Central American ants of the genus *Megalomyrmex* (Hymenoptera: Formicidae): six new species and keys to workers and males. – Zootaxa 3732: 1-82.

Brandão, C.R.F., Diniz, J.L.M. & Feitosa, R.S.M. 2010: The venom apparatus and other morphological characters of the ant *Martialis heureka*. – Papeis Avulsos de Zoologia (São Paulo) 50: 413-423.

Branstetter, M.G., Longino, J.T., Ward, P.S. & Faircloth, B.C. 2017: Enriching the ant tree of life: enhanced UCE bait set for genome-scale phylogenetics of ants and other Hymenoptera. – Methods in Ecology and Evolution 9: 768-776.

Brown, W.L. Jr. 1960: Contributions toward a reclassification of the Formicidae. III. Tribe Amblyoponini (Hymenoptera). – Bulletin of the Museum of Comparative Zoology 122: 143-230.

Brown, W.L. Jr., Gotwald, W.H. Jr. & Levieux, J. 1971: A new genus of ponerine ants from West Africa (Hymenoptera: Formicidae) with ecological notes. – Psyche 77: 259-275.

Brown, W.L. Jr. & Nutting, W.L. 1949: Wing venation and the phylogeny of the Formicidae (Hymenoptera). – Transactions of the American Entomological Society 75: 113-132.

Chen, Z.L., Shi, F.M. & Zhou, S.Y. 2017: First record of the monotypic genus *Opamyrma* (Hymenoptera: Formicidae) from China. – Far Eastern Entomologist 335: 7-11.

Fisher, B.L. & Bolton, B. 2016: Ants of Africa and Madagascar, a guide to the genera. – University of California Press, Berkeley, CA, 503 pp.

Gotwald, W.H. Jr. 1969: Comparative morphological studies of the ants: with particular reference to the mouthparts (Hymenoptera: Formicidae). – Memoirs of the Cornell University Agricultural Experiment Station 408: 1-150.

Hermann, H.R. 1969: The hymenopterous poison apparatus: evolutionary trends in three closely related subfamilies of ants (Hymenoptera: Formicidae). – Journal of the Georgia Entomological Society 4: 123-141.

Hermann, H.R. & Blum, M.S. 1981: Defensive mechanisms in the social Hymenoptera. In: Hermann, H.R. (Ed.): Social insects. Volume 2. – Academic Press, New York, NY, pp. 77-197.

Hermann, H.R. & Chao, J.T. 1983: Furcula, a major component of the hymenopterous venom apparatus. – International Journal of Insect Morphology and Embryology 12: 321-337.

Hermann, H.R., Moser, J.C. & Hunt A.N. 1970: The hymenopterous poison apparatus. X. Morphological and behavioral changes in *Atta texana* (Hymenoptera: Formicidae). – Annals of the Entomological Society of America 63: 1552-1558.

Hölldobler, B., Palmer, J.M., Masuko, K. & Brown, W.L. Jr. 1989: New exocrine glands in the legionary ants of the genus *Leptanilla* (Hymenoptera: Formicidae: Leptanillinae). – Zoomorphology 108: 255-261.

Hsu, P.W., Hsu, F.C., Hsiao, Y. & Lin, C.C. 2017: Taxonomic notes on the genus *Protanilla* (Hymenoptera: Formicidae: Leptanillinae) from Taiwan. – Zootaxa 4268: 117-130.

Inoue, T. & Osatake, H. 1988: A new drying method of biological specimens for scanning electron microscopy: the t-butyl alcohol freeze-drying method. – Archives of Histology and Cytology 51: 53-59.

Keller, R.A. 2011: A phylogenetic analysis of ant morphology (Hymenoptera: Formicidae) with special reference to the poneromorph subfamilies. – Bulletin of the American Museum of Natural History 355: 1-90.

Kubota, H., Yoshimura, J., Niitsu, S. & Shimizu, A. 2019: Morphology of the tentorium in the ant genus *Lasius* Fabricius (Hymenoptera: Formicidae). – Scientific Reports 9: art. 6722.

Kück, P., Garcia, F.H., Misof, B. & Meusemann, K. 2011: Improved phylogenetic analyses corroborate a plausible position of *Martialis heureka* in the ant tree of life. – Public Library of Science One 6: art. e21031.

Kugler, C. 1978: A comparative study of the myrmicine sting apparatus (Hymenoptera, Formicidae). – Studia Entomologica 20: 413-548.

Kugler, C. 1992: Stings of ants of the Leptanillinae (Hymenoptera: Formicidae). – Psyche 99: 103-115.

Kumpanenko, A.S. & Gladun, D.V. 2018: Functional morphology of the sting apparatus of the spider wasp *Cryptocheilus versicolor* (Scopoli, 1763) (Hymenoptera: Pompilidae). – Entomological Science 21: 124-132.

Lange, R., Reinhardt, K., Michiels, N.K. & Anthes, N. 2013: Functions, diversity, and evolution of traumatic mating. – Biological Reviews 88: 585-601.

Liu, S.P., Richter, A., Stoessel, A. & Beutel, R.G. 2019: The mesosomal anatomy of *Myrmecia nigrocincta* workers and evolutionary transformations in Formicidae (Hymenoptera). – Arthropod Systematics & Phylogeny 77: 1-19.

Man, P., Ran, H., Chen, Z. & Xu, Z. 2017: The northern-most record of Leptanillinae in China with description of *Protanilla beijingensis* sp. nov. (Hymenoptera: Formicidae). – Asian Myrmecology 9: art. e009008.

Mason, W.R.M. 1986: Standard drawing conventions and definitions for venational and other features of wings of Hymenoptera. – Proceedings of the Entomological Society of Washington 88: 1-7.

Masuko, K. 1986: Larval hemolymph feeding: a nondestructive parental cannibalism in the primitive ant *Amblyopone silvestrii* (Hymenoptera: Formicidae). – Behavioral Ecology and Sociobiology 19: 249-255.

Masuko, K. 1989: Larval hemolymph feeding in the ant *Leptanilla japonica* by use of a specialized duct organ, the "larval hemolymph tap" (Hymenoptera: Formicidae). – Behavioral Ecolology and Sociobiology 24: 122-132.

Masuko, K. 1990: Behavior and ecology of the enigmatic ant *Leptanilla japonica* Baroni Urbani (Hymenoptera: Formicidae: Leptanillinae). – Insectes Sociaux 37: 31-57.

Masuko, K. 1993: Predation of centipedes by the primitive ant *Amblyopone silvestrii*. – Bulletin of the Association of Natural Science, Senshu University 24: 35-44.

Masuko, K. 2008: Larval stenocephaly related to specialized feeding in the ant genera *Amblyopone*, *Leptanilla* and *Myrmecina* (Hymenoptera: Formicidae). – Arthropod Structure & Development 37: 109-117.

Masuko, K. 2019: Larval hemolymph feeding and hemolymph taps in the ant *Proceratium itoi* (Hymenoptera: Formicidae). – Myrmecological News 29: 21-34.

Ogata, K. 1991: A generic synopsis of the poneroid complex of the family Formicidae in Japan (Hymenoptera). Part 2. Subfamily Myrmicinae. – Bulletin of the Institute of Tropical Agriculture Kyushu University 14: 61-149.

Ogata, K., Terayama, M. & Masuko, K. 1995: The ant genus *Leptanilla*: discovery of the worker-associated male of *L. japonica*, and a description of a new species from Taiwan (Hymenoptera: Formicidae: Leptanillinae). – Systematic Entomology 20: 27-34.

Petersen, B. 1968: Some novelties in presumed males of Leptanillinae (Hymenoptera: Formicidae). – Entomologiske Meddelelser 36: 577-598.

Rabeling, C., Brown, J.M. & Verhaagh, M. 2008: Newly discovered sister lineage sheds light on early ant evolution. – Proceedings of the National Academy of Sciences of the United States of America 105: 14913-14917.

Richter, A., Keller, R.A., Rosumek, F.B., Economo, E.P., Garcia, F.H. & Beutel, R.G. 2019: The cephalic anatomy of workers of the ant species *Wasmannia affinis* (Formicidae, Hymenoptera, Insecta) and its evolutionary implications. – Arthropod Structure & Development 49: 26-49.

Saux, C., Fisher, B.L. & Spicer, G.S. 2004: Dracula ant phylogeny as inferred by nuclear 28S rDNA sequences and implications for ant systematics (Hymenoptera: Formicidae: Amblyoponinae). – Molecular Phylogenetics and Evolution 33: 457-468.

Van Marle J & Piek T. 1986: Morphology of the venom apparatus. In: Piek, T. (Ed.): Venoms of the Hymenoptera. – Academic Press, New York, NY, pp. 17-44.

Ward, P.S. & Fisher, B.L. 2016: Tales of dracula ants: the evolutionary history of the ant subfamily Amblyoponinae (Hymenoptera: Formicidae). – Systematic Entomology 41: 683-693.

Wheeler, G.C. & Wheeler, J. 1965: The ant larvae of the subfamily Leptanillinae (Hymenoptera, Formicidae). – Psyche 72: 24-34.

Wheeler, G.C. & Wheeler, J. 1989: The larva of *Leptanilla japonica*, with notes on the genus (Hymenoptera: Formicidae: Leptanillinae). – Psyche 95: 185-189.

Yamada, A. & Eguchi, K. 2016: Description of the male genitalia of *Pristomyrmex punctatus* (Smith, 1860) (Hymenoptera: Formicidae: Myrmicinae). – Asian Myrmecology 8: 1-8.

Yamane, S., Bui, T.V. & Eguchi, K. 2008: *Opamyrma hungvuong*, a new genus and species of ant related to *Apomyrma*. – Zootaxa 1767: 55-63.

Yamane, S. & Jaitrong, W. 2019: Discovery of the male of the ant genus *Anillomyrma* (Emery, 1913) (Hymenoptera: Formicidae: Myrmicinae). – Japanese Journal of Systematic Entomology 25: 9-14.

Yoshimura, M. & Fisher, B.L. 2011: A revision of male ants of the Malagasy region (Hymenoptera: Formicidae): key to genera of the subfamily Dolichoderinae. – Zootaxa 2794: 1-34.